

1 **Multi-year emission of carbonaceous aerosols from cooking, fireworks burning,**
2 **sacrificial incenses, joss paper burning, and barbecue and the key driving forces in**
3 **China**

4 **Yi Cheng**^{1,2}, **Shaofei Kong**^{1,2*}, **Liquan Yao**^{1,2}, **Huang Zheng**^{1,2}, **Jian Wu**^{1,2}, **Qin Yan**^{1,2}, **Shurui Zheng**
5 ^{1,2}, **Yao Hu**^{1,2}, **Zhenzhen Niu**^{1,2}, **Yingying Yan**¹, **Zhenxing Shen**³, **Guofeng Shen**⁴, **Dantong Liu**⁵,
6 **Shuxiao Wang**⁶, and **Shihua Qi**²

7 ¹ Department of Atmospheric Science, School of Environmental Studies, China University of Geoscience,
8 Wuhan, China

9 ² Department of Environment Science and Engineering, School of Environmental Studies, China University
10 of Geoscience, Wuhan, China

11 ³ Department of Environmental Science and Engineering, School of Energy and Power Engineering, Xi'an
12 Jiaotong University, Xi'an, China

13 ⁴ Laboratory for Earth Surface Process, College of Urban and Environmental Sciences, Peking University,
14 Beijing, China

15 ⁵ Department of Atmospheric Science, School of Earth Science, Zhejiang University, Hangzhou, China

16 ⁶ State Key Joint Laboratory of Environmental Simulation and Pollution Control, School of Environment,
17 Tsinghua University, Beijing, China

18 Corresponding to: Shaofei Kong (kongshaofei@cug.edu.cn)

19

20 **Abstract**

21 There has been controversy about the air pollutants emitted from sources closely related to people's
22 daily life (such as cooking, fireworks burning, sacrificial incenses and joss paper burning, and barbecue,
23 named as five missing sources, FMS) impacting the outdoor air quality to what extent. Till now, there is no
24 emission estimation of air pollutants from FMS, as the missing of both activity dataset and emission factors.
25 We attempted to combine the questionnaire data, various statistical data, and data of points of interest to
26 obtain a relatively complete set of activity data. The emission factors (EFs) of carbonaceous aerosols were
27 tested in our lab. Then, the emission inventories of carbonaceous aerosol with a high spatial-temporal
28 resolution for FMS were established firstly, and the spatial variation trend and driving forces were discussed.
29 From 2000 to 2018, organic carbon (OC) emissions were in the range of 4268–4919 t. The OC emission
30 from FMS was 1.5–2.2 % of its total emission in China. The emissions of black carbon, element carbon
31 (EC), and brown carbon absorption cross-section (ACS_{BrC}) emissions from FMS were in the ranges of 22.6–
32 43.9 t, 213–324 t, and 14.7–35.6 Gm^2 , respectively. Their emissions tended to concentrate in special periods
33 and areas. The OC emission intensities in central urban areas were 3.85–50.5 times that of rural areas due to
34 the high density of human activities. While the ACS_{BrC} emissions in rural regions accounted for 63.0–79.5%
35 of the total emission result from uncontrolled fireworks burning. A mass of fireworks burning led to
36 extremely higher ACS_{BrC} and EC emissions on Chinese New Year's eve, as 1444 and 262 times their
37 corresponding yearly average values. Significant ($p < 0.01$) correlations between human incomes and
38 pollutant emissions were found, while they were positive ($r = 0.94$) and negative ($r = -0.94$) for urban and
39 rural regions, indicating the necessity of regulating human lifestyle and increasing income for urban and
40 rural peoples, respectively. This study provided the first-hand data for identifying the emissions, variation
41 trends and impacting factors of FMS, which is helpful for modeling works on air quality, climate effect, and
42 human health risks at specific periods or regions and for modifying their emission control policies. The data
43 in this work could be found at <https://doi.org/10.6084/m9.figshare.19999991.v2> (Cheng et al., 2022).

44 **Keywords:** Carbonaceous aerosols; Sources related to human activities; Emission inventory; Spatial-
45 temporal variation; Driving force

46

47 **1 Introduction**

48 China has experienced a period of serious air pollution, which produces a great health impact on
49 residents (Zheng et al., 2018; Zhang et al., 2019, 2020b; Tong et al., 2020). Carbonaceous aerosols (CA),
50 emitted from incomplete burning, include organic carbon (OC) and black carbon (BC, or element carbon,
51 EC), and they have attracted wide attention due to their adverse impacts on air quality, human health and
52 climate (Venkataraman et al., 2005; Ramanathan & Carmichael, 2008; Bond et al., 2013). The optical
53 properties of CA (especially brown carbon, BrC) are complex and mutative, which is also one of the
54 important factors affecting the global radiation balance (Feng et al., 2013; Laskin et al., 2015).

55 Several sources closely related to traditional human activities were potential emission sources of CA,
56 such as the burning of sacrificial incense and joss paper, traditional Chinese barbecue, Chinese style cooking,
57 and fireworks burning. The estimation of air pollutants from these sources was missing in the previous
58 emission inventory, and they were defined as five missing sources (FMS) in this study. FMS can lead to a
59 dramatic impact on ambient quality and human health in a short period or a specific region (Chiang & Liao,
60 2006; Wu et al., 2015; Kong et al., 2015; Ho et al., 2016; Wang et al., 2017; Lai & Brimblecombe, 2020).
61 For example, fireworks burning could contribute 60.1 % of PM_{2.5} during the Chinese Lunar New year's eve
62 in Nanjing, and sacrificial sources like sacrificial incense and joss paper burning could contribute 17.5% of
63 atmospheric PAHs in Chu-Shan, and 9.6% of PCDD/F in Taipei (Lin et al., 2008; Kong et al., 2015; Ho et
64 al., 2016). Recently, with the strengthened control of combustion-related sources, the important role of
65 cooking emissions on affecting air quality was gradually visible in densely populated downtown areas.
66 Cooking organic aerosols contributed to 15–34% of total OC and 6–9% of total PM_{2.5} in a downtown site in
67 Shanghai (Huang et al., 2022) and 31% of total organic aerosols in Beijing in winter (Hu et al., 2022). The
68 existing studies on FMS were mainly based on the ambient air monitoring datasets at certain sites or certain
69 periods (See & Balasubramanian, 2011; Wu et al., 2015; Shen et al., 2017; Lao et al., 2018; Tanda et al.,
70 2019; Yao et al., 2019; Hu et al., 2021; Huang et al., 2021). Till now, no studies can provide their
71 contributions quantitatively on a large scale as the scare of emission inventory, which limited the identification
72 of their contributions in various regions or periods.

73 There also existed extensive queries that are these conclusions tenable as they were identified through
74 models or ambient monitoring data, but not from their real emission estimation. In China, the differences in

75 population and economy between urban and rural areas are increasing (Meng et al., 2019), and the
76 efficiencies and necessity of air quality control policies for FMS in urban and rural areas need to be assessed.
77 For instance, fireworks burning was generally banned in the central urban region, while suburbs and rural
78 regions were affected less by the policy. The cooking smokes needed to be purified in city centers, while in
79 suburban and rural areas, the policy may be not strictly executed or it is even not necessary. Such deviations
80 in policy establishment and implementation could ultimately drive the differences in the distribution of air
81 pollutant emissions, which have not been addressed yet.

82 The emission inventory is the base for the quantitative description of anthropogenic pollutant emissions
83 (Li et al., 2017). The combination of the chemical transport models and high-resolution emission inventory
84 was paramount for understanding anthropogenic perturbations' impacts on the atmosphere, and for assessing
85 corresponding air pollution control strategies (Janssens-Maenhout et al., 2019; McDuffie et al., 2020). The
86 lack of emission inventories limits the large-scale model simulation, the optimization of corresponding
87 control measures, and the settlement of related disputes. In our previous work, Wu et al. (2021) have
88 established an emission inventory of levoglucosan which included the emissions from FMS (Wu et al., 2021).
89 There were no other emission inventories of FMS reported, to the best of our knowledge.

90 To sum up, this study aimed to develop a methodological framework for establishing an emission
91 inventory of FMS, including the methods of various activity data acquisition, emission factors monitoring,
92 uncertainty assessment, and spatial-temporal allocation. The activity data were obtained based on household
93 investigation, statistic data, points of interest (POI), etc. The emission factors were monitored through a
94 unique emission monitoring test platform, especially for fireworks burning in our lab. Then a high spatial
95 (~1 km) and temporal resolution (1 day for special festivals, and 1 month for the rest) emission inventory
96 was first established. The multi-year spatiotemporal variation of CA emissions from these sources was
97 analyzed and compared with other types of sources. Optimization pollution control measures were proposed
98 for these types of sources. The study provides a methodology for establishing an emission inventory of air
99 pollutants from sources closely related to human activities. Other air pollutants emissions could also be
100 estimated in the future. The emission inventory obtained here could also provide the basic inputs for
101 corresponding modeling works.

2 Methodology

2.1 Combustion tests for emission factors

The combustion tests for FMS were performed with two custom-made combustion chambers. One of them had an explosion-proof function and it was used in fireworks burning experiments. Another one was used in sacrificial incense, joss paper, barbecue, and cooking emission experiments. A dilution sampling system (Dekati FPS-4000, Finland) was employed to dilute the smoke. The smokes were diluted about 16–30 times and aged for about 30 s in a residence chamber. The sampling system has been utilized in residential fuel combustion experiments (Cheng et al., 2019; Yan et al., 2020; Zhang et al., 2021b; Wu et al., 2021). Thirty-eight events were tested in this experiment, including 6 trials of sacrificial incense combustion (abbreviations of materials: red incense: RI; environmental incense: EI; high incense: HI), 6 trials of joss paper burning (red-printed paper: RP; small sacrificial paper: SP; large sacrificial paper: LP), 10 trials of fireworks burning (firecrackers: FC; fountain fireworks: FF; handheld fireworks: HF; handheld fountain: HT; spin fireworks: SF), 8 trials of barbecue (chicken: CK; beef: BF, lamb: LB; pork: PK), and 8 trials of cooking (cooking of meat: MT1; cooking of meat and pepper: MT2; cooking of meat and garlic: MT3; cooking of meat, pepper, and garlic: MT4). The experiment materials were shown in **Figure S1**.

After diluted, the OC and EC in the smokes were detected with an online carbonaceous aerosol analyzer. It was developed by the Key Laboratory of Environmental Optics & Technology (Anhui Institute of Optics and Fine Mechanics, CAS) based on the thermal-optical method (Ding et al., 2014). The analyzer showed reliable stability and repeatability. More details on the online carbonaceous aerosol analyzer can be found in **Text S1**. A dual-spot Aethalometer (Model AE33, Magee Scientific, USA) was employed to measure BC concentration and particulate optical properties (Drinovec et al., 2015). The experiment system was shown in **Figure S2**.

2.2 Calculation of emission factors and optical properties

The emission factors of OC, EC, and BC were calculated by equation (1):

$$EF_{ij} = \frac{v \times m_{ij} \times r}{v_0 \times M_j} \quad (1)$$

where i and j denoted pollutant and fuel; EF was the emission factor (mg kg^{-1}); v was the flue gas flow (L min^{-1}); v_0 was the sampling flow (L min^{-1}); m was the mass of the pollutant detected by the instruments (mg); r was the dilution ratio; M was the mass of the material used in each tail of experiments

(kg) (Cheng et al., 2019; Yan et al., 2020).

All filter-based optical measurements will be confronted with the underestimation caused by the loading effect (Drinovec et al., 2015). The loading compensation could be calculated based on dual-spot measurements. The detailed calculation process was referred to Drinovec et al. (2015). There was inferior dependence of BC particles on light absorption in different light wavelengths. The absorption Ångström exponent (AAE) was an exceptional parameter to describe this dependence, as shown in equations (2) and (3):

$$b_{abs} \sim \lambda^{-AAE} \quad (2)$$

$$AAE = - \frac{\ln \left(\frac{b_{abs}(\lambda_1)}{b_{abs}(\lambda_2)} \right)}{\ln \left(\frac{\lambda_1}{\lambda_2} \right)} \quad (3)$$

where λ was the wavelength; b_{abs} denoted the total light absorption coefficient (Tian et al., 2019), which could be calculated by equation (4) (Zotter et al., 2017):

$$BC = b_{abs}(\lambda) / MAC(\lambda) \quad (4)$$

where MAC was the mass absorption cross-section, referring to the Aethalometer manufacturer.

As shown in equation (5), the b_{abs} of CA was aroused by BC and BrC. To calculate the $b_{abs}(\lambda, BC)$ at each wavelength, equation (6) was introduced. The AAE_{BC} was determined as 1.0 according to previous studies (Tian et al., 2019; Liakakou et al., 2020). $f_{BrC}(\lambda)$ (equation (7) was utilized to estimate the fraction of BrC light absorption ($b_{abs}(\lambda, BrC)$) in total light absorption ($b_{abs}(\lambda)$).

$$b_{abs}(\lambda) = b_{abs}(\lambda, BC) + b_{abs}(\lambda, BrC) \quad (5)$$

$$b_{abs}(\lambda, BC) = b_{abs}(880) \times \left(\frac{\lambda}{880} \right)^{-AAE_{BC}} \quad (6)$$

$$f_{BrC}(\lambda) = 100\% \times b_{abs}(\lambda, BrC) / b_{abs}(\lambda) \quad (7)$$

Due to the complicated chemical properties of BrC, it was difficult to measure the accurate concentration of BrC in flue gases. Previous studies have developed a peculiar EF called absorption emission factor (AEF), as shown in equation (8) (Martinsson et al., 2015; Tian et al., 2019; Zhang et al., 2020c). Most studies modeled the direct radiative forcing of BrC with its mass concentration and mass absorption efficiency (MAE) as the input parameters. While the mass concentration and the total mass of BrC in the atmosphere were still unclear, and the MAE values in the range of 0.08–3.8 m² g⁻¹ were also variable (Park

et al., 2010; Feng et al., 2013; Wang et al., 2014b; Zhang et al., 2020a). An inventory established by AEF as the following equation could avoid the deviation raised by the mass concentration and MAE of BrC (Tian et al., 2019).

$$AEF_{ij} = \frac{\sum_{t_0}^{t_{sample}} (b_{abs_{ij}} \times r \times v)}{M_j} \quad (8)$$

2.3 Acquisition of activity data

Data on the activity of sources directly affected the uncertainties of emission inventory, and an accurate estimate of FMS consumption was a crucial prerequisite. Statistics on direct consumption of FMS were scarce. Then multiple activity data and proxy variables were adopted, including the statistical yearbooks of each province in China, datasets of POI (Text S2, Figure S3), and rural household investigation data in our group (Text S3).

The original consumptions of sacrificial incenses, joss paper and fireworks were from a household investigation. We got the per capita consumption of sacrificial incenses, joss paper, and fireworks in each province. The data were adjusted to overcome the problem of insufficient sample size. In China, sacrificial activities mean honoring ancestors, and they mainly take place in temples or graveyards. China is a mountainous country with rolling terrain. Most of the inhabitants of non-plain areas chose hills that might cover vegetation as the site of graveyards. The data on the consumption of sacrificial incenses and joss paper will be revised based on the number of temples (data from POI) and frequency of forest fires caused by sacrifices to the total forest fires (data from China Forestry Statistical Yearbook), as shown in equation (9):

$$Cs_{adj,province} = Cs_{inv,province} \times \left(\frac{Nt_{province}/POP_{province}}{2 \times Nt_{nation}/POP_{nation}} + \frac{Fs_{province}/Ft_{province}}{2 \times Fs_{nation}/Ft_{nation}} \right) \quad (9)$$

where Cs was the consumption of sacrificial incenses or joss paper per capita; Nt was the number of temples; POP was the population, which came from the statistical yearbook of each province; Fs was the forest fires raised by sacrificial activities; Ft was the forest fires raised by all anthropogenic activities; adj represented the data after adjusted; inv represented the data from the household investigation; $province$ represented the data of each province; $nation$ represented the data of the entire nation.

The fireworks consumption amounts will be revised based on the number of retail shops of fireworks (data from POI) and provincial fireworks export volume (statistical data), as shown in equation (10):

$$Cf_{adj,province} = Cf_{inv,province} \times \left(\frac{Ns_{province}/POP_{province}}{2 \times Ns_{nation}/POP_{nation}} + \frac{Ve_{province}/POP_{province}}{2 \times Ve_{nation}/POP_{nation}} \right) \quad (10)$$

where C_f was the consumption of fireworks per capita; N_s was the number of retail shops of fireworks; Ve was the export volume of fireworks (data from China Light Industry Yearbook). In addition, the consumptions (C) of sacrificial incenses, joss paper, and fireworks at the municipal level were calculated by combining the POI data and the consumptions at the provincial level, as shown in equation (11).

$$C_{adj,city} = C_{inv,province} \times \frac{N_{city}/POP_{city}}{N_{province}/POP_{province}} \quad (11)$$

where N represented the number of temples or firework shops.

The original meats consumption per capita came from the statistical yearbook of each province. While the methods and radii of different provincial statistical yearbooks showed differences. Part of the municipal level statistics was missing. To complement the missing data, municipal per capita consumption expenditure was introduced. The logarithmic relationship between per capita consumption expenditure and provincial per capita meat consumption was adopted to complement municipal per capita meat consumption, as shown in equation (12):

$$y = a \times \ln x + b \quad (12)$$

where x represented the provincial per capita consumption expenditures in 2000–2018; y represented provincial per capita meat consumption in 2000–2018. Parameters a and b were fit-out for each province ($r = 0.60, p < 0.01$). The parameters a and b of the province where each city is located, and the per capita consumption expenditure of the city were substituted into equation (12) to calculate the municipal per capita meat consumption.

2.4 Calculation of the emissions

Since some cities have established policies to forbid sacrificial incense, joss paper, and fireworks burning in the main urban area, and such policies were inoperative in non-urban regions. According to our survey, the policies on forbidden sacrificial incense and joss paper were relatively vague. We assumed that if one city forbade fireworks burning, then the burning of sacrificial incense and joss paper was also banned. The total emissions E from sacrificial incense, joss paper, and fireworks were calculated by equation (13):

$$E = \sum (POP_{urban,k} \times C_{urban,k} \times FB_k + POP_{non-urban,k} \times C_{non-urban,k}) \times EF \quad (13)$$

where k denoted the different cities; *urban* and *non-urban* represented urban regions and non-urban regions (rural regions); POP was the population; C was the per capita consumption; EF was the emission factor. $FB = 0$ or 1 depended on whether the burning of sacrificial incense, joss paper, and

firework was forbidden in urban regions. Unfortunately, there was no such detailed consumption data that involved the fuel types of sacrificial incense, joss paper, and fireworks. Thus, for the calculation of emission from sacrificial incense, joss paper, and fireworks, mean EFs were utilized here.

Emissions from barbecue were calculated by formula (14):

$$E = \sum (POP_{urban,k} \times MC_{urban,k} + POP_{non-urban,k} \times MC_{non-urban,k}) \times \frac{T_{BBQ,k}}{T_{total,k}} \times OP \times EF \quad (14)$$

where MC was the meat consumption mass per capita; T_{BBQ} was the number of restaurants specializing in barbecue; T_{total} was the total number of restaurants. The numbers of restaurants were calculated by using POI data. OP was the percentage of meals eaten out (data from the National Institute for Nutrition and Health, Chinese Center for Disease Control and Prevention). In this study, we assumed that barbecue was a kind of eating out.

Emission from cooking was the sum of the emissions from residential cooking and from the catering industry. They were calculated by formulas (15) and (16):

$$E_{RC} = \sum (POP_{urban,k} \times MC_{urban,k} + POP_{non-urban,k} \times MC_{non-urban,k}) \times \left(1 - \frac{T_{BBQ,k}}{T_{total,k}}\right) \times (1 - OP) \times EF \times RE_{RC,k} \quad (15)$$

$$E_{CI} = \sum (POP_{urban,k} \times MC_{urban,k} + POP_{non-urban,k} \times MC_{non-urban,k}) \times \left(1 - \frac{T_{BBQ,k}}{T_{total,k}}\right) \times OP \times EF \times RE_{CI,k} \quad (16)$$

where E_{RC} was the emission from the residential cooking and E_{CI} was the emission from the catering industry; RE was the removal efficiency. The removal efficiency of the catering industry (RE_{CI}) was from the national standard (GB 18483-2001). The removal efficiency of residential cooking activity (RE_{RC}) was calculated using the popularizing rate of the range hood (data from China Statistical Yearbook) and removal efficiency of the range hoods (GB/T 17713-2011).

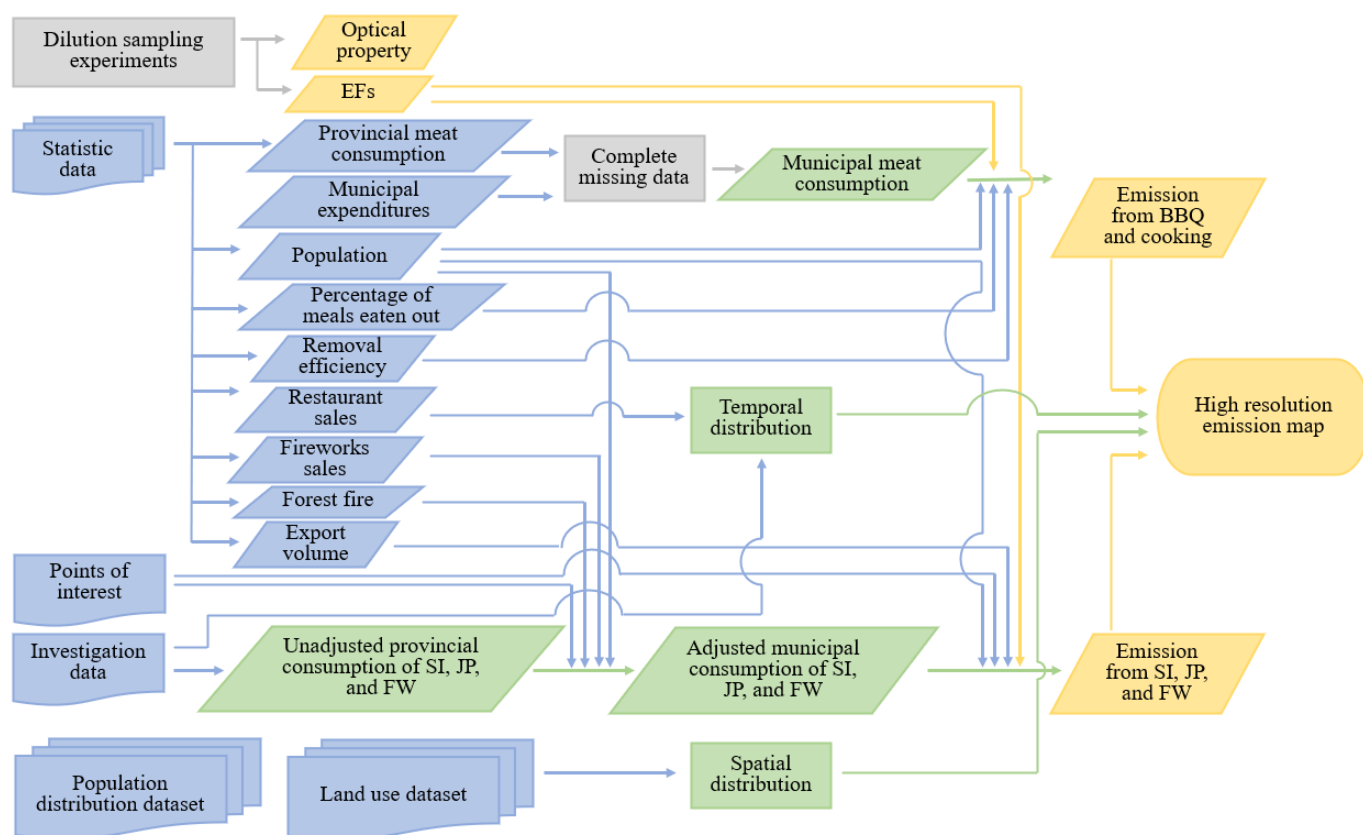
A Monte Carlo simulation was employed to analyze the uncertainties of the emission inventory (Wu et al., 2018). The simulation was executed 10000 times. The uncertainties of activity data were set as 0.2 or 0.5 (Table S1), and the uncertainties of EFs came from the actual measurements. The result of uncertainty was shown in Table S2.

2.5 Spatial-temporal distribution of emissions

As above-mentioned, the emissions from rural and urban FMS activity might differ greatly. During the process of spatial allocation, this difference must be emphasized. We were tempted to use GIS data for the classification of land use to divide urban and non-urban regions (Gong et al., 2019, 2020). Based on this

239 method, we got the data on the population distribution (data from www.worldpop.org,
 240 10.5258/SOTON/WP00674) in urban and rural regions and constructed the emission map from FMS (Text S4).

241 The temporal allocation methods for FMS were also specific. For calculating the annual trends of
 242 emissions, statistical data including annual fireworks sales (data from the statistic of the Ministry of
 243 Emergency Management of the PRC) and annual restaurant sales (data from https://data.stats.gov.cn/) were
 244 used. The monthly trends of sacrificial incenses, joss paper, and fireworks burning were calculated with data
 245 from household investigations. We believed that the activities of these sources are mainly concentrated on
 246 five traditional Chinese festivals, including Chinese New Year’s Eve (CNE), Chinese Spring Festival (CSF),
 247 Spring Lantern Festival (LF), Qingming Festival (QF), and Zhongyuan Festival (ZF) (Text S5). We
 248 calculated the percentage of incense, joss paper, and fireworks that burned during these festivals, and spread
 249 the excess to other days. The monthly trends of barbecue and cooking emissions were calculated by using
 250 the monthly restaurant sales in each province (data from https://data.stats.gov.cn/). It should be noted that
 251 the above methods were alternatives due to the lack of direct statistical data, and the methods can be
 252 improved in the future.



253

254 **Figure 1** Methodological framework for establishing a high-resolution emission inventory for FMS.

255 **3 Results and discussion**

256 **3.1 Emission characterization and light absorption properties**

257 The EFs obtained from the 38 tests were shown in **Table 1**. The mean EF_{OC} of sacrificial incense,
258 barbecue, joss paper, fireworks burning, and cooking were $32.6 \pm 12.6 \text{ mg kg}^{-1}$, $33.2 \pm 13.5 \text{ mg kg}^{-1}$, $41.9 \pm$
259 27.8 mg kg^{-1} , $51.9 \pm 45.5 \text{ mg kg}^{-1}$, and $159 \pm 34.0 \text{ mg kg}^{-1}$, respectively. While the EF_{EC} and EF_{BC} showed
260 different tendencies. Barbecue exhibited higher EF_{EC} ($5.13 \pm 5.23 \text{ mg kg}^{-1}$) and EF_{BC} ($69.6 \pm 79.5 \text{ mg kg}^{-1}$)
261 than those of sacrificial incense (EF_{EC}: $0.17 \pm 0.07 \text{ mg kg}^{-1}$, EF_{BC}: $1.80 \pm 0.92 \text{ mg kg}^{-1}$), joss paper ($2.25 \pm$
262 2.47 mg kg^{-1} , $3.79 \pm 2.23 \text{ mg kg}^{-1}$), cooking ($0.005 \pm 0.001 \text{ mg kg}^{-1}$, $1.54 \pm 0.17 \text{ mg kg}^{-1}$), and fireworks
263 burning ($2.57 \pm 5.37 \text{ mg kg}^{-1}$, $14.8 \pm 17.3 \text{ mg kg}^{-1}$). Multiple factors, such as fuel properties (Chen et al.,
264 2009; Shen et al., 2014; Cheng et al., 2019), combustion condition (Cheng et al., 2019), and stove properties
265 (Shen et al., 2014; Chen et al., 2015), affected the emission of CA from combustion sources. Similarly, CA
266 emissions from FMS were dominated by diverse factors. Results in previous studies were also applicable in
267 this study. For example, the emissions from environmental or aromatic incense were lower (Lee and Wang,
268 2004; Lui et al., 2016), and cooking fatty pork generated higher emissions (Saito et al., 2014). In addition,
269 the previous study showed higher EF_{OC} (0.779 g kg^{-1}) and EF_{EC} (0.339 g kg^{-1}) for sacrificial offerings
270 (Zhang et al., 2019b). The huge differences in EFs were highly possible (Liu et al., 2015), and more detailed
271 research is needed to expand the datasets of EFs for FMS in the future.

272

Table 1 BC, OC, and EC emission factors for five missing sources (FMS) (mg kg^{-1}).

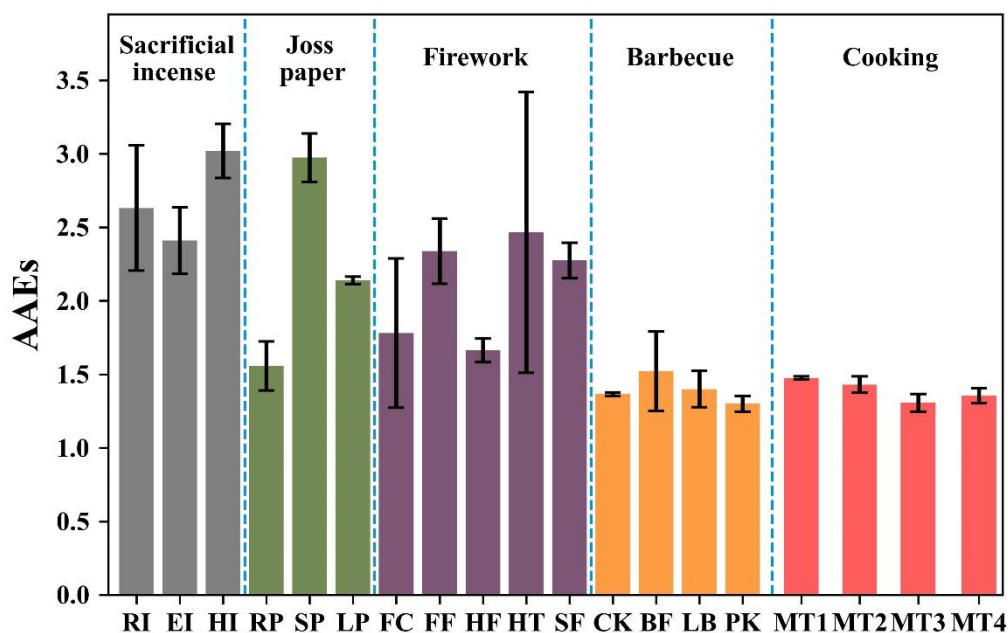
Sources	Materials*	BC	OC	EC
Sacrificial incense	RI	3.09±0.05	49.2±6.39	0.23±0.07
	EI	1.24±0.17	27.3±2.63	0.17±0.02
	HI	1.07±0.04	21.4±2.06	0.10±0.02
Joss paper	RP	6.27±1.59	35.5±5.59	0.97±0.10
	SP	1.65±0.41	14.6±1.64	0.64±0.50
	LP	3.45±1.18	75.5±19.2	5.12±2.28
Fireworks	FC	3.56±0.32	8.72±0.08	0.14±0.03
	FF	2.89±0.88	5.86±1.28	0.06±0.03
	HF	23.0±8.63	124±29.2	9.79±8.49
	HT	7.49±0.20	65.7±10.5	2.39±1.76
	SF	37.3±22.8	55.1±0.66	0.48±0.29
Barbecue	CK	1.66±0.30	21.5±1.11	0.15±0.02
	BF	37.2±24.4	28.6±8.85	3.78±2.28
	LB	48.5±17.7	32.2±6.35	4.21±0.58
	PK	191±59.5	50.5±12.2	12.4±4.93
Cooking	MT1	1.79±0.04	127	0.003
	MT2	1.54±0.01	124	0.004
	MT3	1.34±0.05	181	0.007
	MT4	1.48±0.07	203	0.007

274 *: Abbreviations of fuels: RI: red incense; EI: environmental incense; HI: high incense; RP: red-printed paper; SP:
 275 small sacrificial paper; LP: large sacrificial paper; FC: firecrackers; FF: fountain fireworks; HF: handheld fireworks; HT:
 276 handheld fountain; SF: spin fireworks; CK: chicken; BF: beef, LB: lamb; PK: pork; MT1: cooking of meat; MT2: cooking
 277 of meat and pepper; MT3: cooking of meat and garlic; MT4: cooking of meat, pepper, and garlic. FMS: five missing sources.

278

279 To quantify the light absorption properties of emissions from FMS, AAEs (370-880 nm) were calculated
 280 (**Figure 2**). The average AAEs of FMS were in the range of 1.26–3.15. The mean AAE of sacrificial incenses
 281 (2.69 ± 0.36) was slightly higher compared to joss paper (2.22 ± 0.65), fireworks burning (2.10 ± 0.50),
 282 barbecue (1.40 ± 0.14), and cooking (1.39 ± 0.08). The AAEs in 370-880 nm wavelength of woody fuel
 283 burning (1.0–2.7) (Martinsson et al., 2015; Zhang et al., 2020a, 2021c), crop residues burning (1.5–3.25)
 284 (Tian et al., 2019; Zhang et al., 2020c, 2021a), coal combustion (1.1–2.5) (Tian et al., 2019; Zhang et al.,
 285 2021a), and engines (1.1–2.4) (Corbin et al., 2018) were comparable to our results. $\text{AAE} > 1$ indicates that
 286 there existed BrC in aerosols (Saleh et al., 2013; Sun et al., 2017). Thus, it is necessary to investigate BrC

287 emission characteristics and the contribution of BrC to the total light absorption from various sources.
 288



289
 290 **Figure 2** The absorption Ångström exponents (370-880 nm) of FMS.

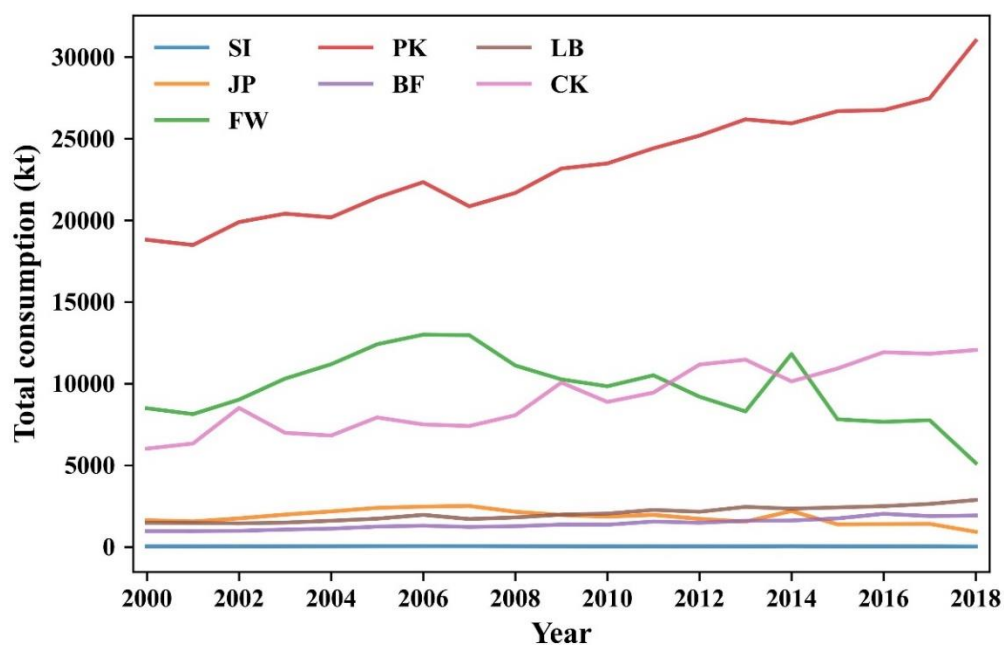
291
 292 We have calculated f_{BrC} to estimate the light absorption ability of BrC in aerosols (**Figure S4**). f_{BrC}
 293 showed a decreasing tendency toward the long wavelengths, which proved the understanding that the light
 294 absorption ability of BrC had stronger spectral dependence than that of BC (Sun et al., 2017). At 370 nm
 295 wavelength, f_{BrC} of sacrificial incense, joss paper, fireworks, barbecue, and cooking were $71.5 \pm 5.32\%$, 58.4
 296 $\pm 24.0\%$, $57.6 \pm 9.36\%$, $28.7 \pm 6.19\%$, and $29.2 \pm 4.30\%$, respectively. f_{BrC} of cooking sources (22.9–37.4%
 297 with an average of 29.0%) like barbecue and cooking seemed to be much lower than other combustion
 298 sources (34.8–82.7% with an average of 61.6%). f_{BrC} were 47% for coal combustion at 355 nm wavelength
 299 (Sun et al., 2017), and 68–85% for biomass burning at 370 nm (Tian et al., 2019). As some emission sources
 300 were neglected, the particulate absorption and warming effect contributed by BrC may be underestimated in
 301 former modeling works (Laskin et al., 2015).

302 Furthermore, the AEF of BrC and BC have been calculated, as shown in **Figure S5**. As the wavelength
 303 increased, the AEFs showed a decreasing trend. When $\lambda=370$ nm, AEF_{BrC} from fireworks burning was the

304 highest, as $2.65 \pm 3.23 \text{ m}^2 \text{ kg}^{-1}$, followed by barbecue ($0.45 \pm 0.49 \text{ m}^2 \text{ kg}^{-1}$), joss paper ($0.19 \pm 0.21 \text{ m}^2 \text{ kg}^{-1}$),
 305 sacrificial incenses ($0.15 \pm 0.10 \text{ m}^2 \text{ kg}^{-1}$), and cooking ($0.012 \pm 0.004 \text{ m}^2 \text{ kg}^{-1}$). At 370 nm, the AEF_{BrC} of
 306 coal combustion and biomass burning have been reported as $14.3\text{--}46.6 \text{ m}^2 \text{ kg}^{-1}$ and $2.01\text{--}24 \text{ m}^2 \text{ kg}^{-1}$
 307 (Martinsson et al., 2015; Tian et al., 2019), which were 1–3 order of magnitude higher than those of FMS.

308 3.2 Characterization of activity

309 The total consumption of FMS was shown in **Figure 3**. In 2018, 16.5 kt, 919 kt, and 5139 kt of sacrificial
 310 incenses, joss paper, and fireworks were consumed in China. 30996 kt, 2872 kt, 1920 kt, and 12057 kt of
 311 pork, beef, lamb, and chicken were consumed. The total consumption amount of FMS was about 26.4% of
 312 the residential coal consumption in China (Peng et al., 2019). The consumptions of sacrificial incense, joss
 313 paper, and fireworks were highest in Shandong (394 kt) and Sichuan (470 kt). Apart from lamb, Guangdong
 314 province has the largest consumption of three kinds of meats (6197 kt), and the province with the largest
 315 consumption of lamb was Xinjiang (361 kt). The consumption of FMS can be a reflection of the local
 316 customs. For example, lamb consumption in Xinjiang was the highest in China. The reason may be that
 317 Xinjiang is the main producing area of lamb, one of the five pastoral areas in China, and Xinjiang's ethnic
 318 structure makes mutton a dominant part of the daily diet (Xu et al., 2018).



319
 320 **Figure 3** The total consumption of FMS during 2000–2018 in China (Abbreviation: SI: sacrificial incense; JP: joss paper;
 321 FW: fireworks; PK: pork; BF: beef; LB: lamb; CK: chicken).

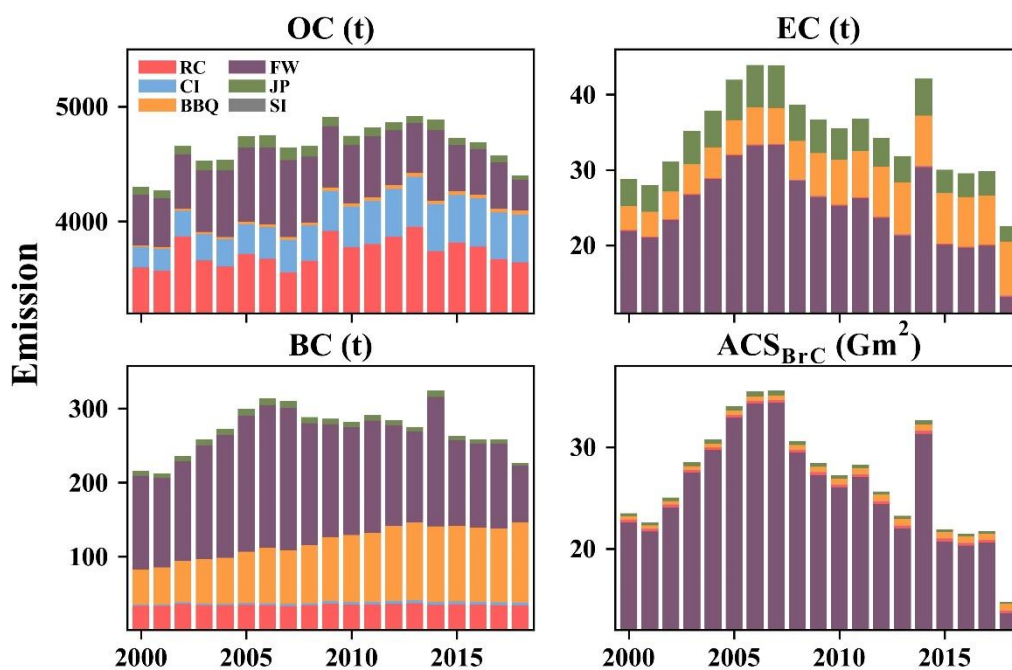
322 The FMS consumptions in most cities were at low levels. The top 30 cities (about 8% of the total
323 number of cities) with the largest fireworks consumption contributed 41.8% of the national consumption
324 (**Figure S6**). These cities have higher population densities, and the control measures for fireworks were not
325 yet in place. Per capita fireworks consumption in 52% of the cities was less than 5 kg yr⁻¹, and the mass of
326 a common firecracker can exceeds 5 kg. As shown in **Figure S7**, the distribution pattern of per capita
327 consumption of sacrificial incenses and joss paper was similar to that of fireworks. The differences in meat
328 consumption between cities were relatively smaller. The top 30 cities with the largest pork consumption only
329 contributed 30.8% of the national consumption. The lowest per capita pork consumption was only 2.31 kg
330 yr⁻¹ and the highest was 45.6 kg yr⁻¹ (**Figure S7**). While 71.9% of the cities had per capita pork consumption
331 of 10–30 kg yr⁻¹. From 2000 to 2018, the consumption of four types of meat increased by 49.3%, and the
332 trends of increased meat consumption were similar to a previous study (Batis et al., 2014). While the
333 consumption of sacrificial incense, joss paper, and fireworks showed a trend of increasing first and then
334 decreasing.

335 **3.3 CA emission from FMS in China**

336 **3.3.1 Multi-year variation**

337 In 2000–2018, OC, EC, BC, and BrC absorption cross-section (ACS_{BrC}, in 370 nm wavelength)
338 emissions from FMS were 4268–4919 t, 22.6–43.9 t, 213–324 t, and 14.7–35.6 Gm², respectively (**Figure**
339 **4**). Severe air pollution over the past decade has led China to enact a series of policies to limit emissions
340 from various sources. Thus, the total CA emission in China presented approximately monotonically
341 decreased tendencies. During 2010–2017, the total OC and BC emissions in China decreased from 3.2 Tg
342 and 1.7 Tg to 2.1 Tg and 1.3 Tg, mostly contributed by residential sources (76.9–80.3% of OC, 41.8–51.5%
343 of BC) (<http://meicmodel.org>, Li et al., 2017; Zheng et al., 2018). The emission from FMS showed different
344 variation tendencies compared with these above sources. 82.7–92.3% of OC emissions came from cooking
345 (**Figure S8**). Due to the increased meat consumption (increased by 49%) and the popularizing rates of range
346 hoods (increased by 43.0%), the OC emissions from FMS increased by 14.4% before 2013 and then
347 decreased by 10.6%. The EC, BC, and ACS_{BrC} emissions showed similar tendencies. From 2000 to 2006,
348 EC, BC, and ACS_{BrC} emissions from FMS increased by 52.3%, 45.4%, and 51.2%, respectively. Then they
349 decreased by 48.7%, 27.8%, and 58.4% in 2006–2018. Fireworks burning was one of the main contributors
350 to CA emissions from FMS, which contributed 58.6–76.0%, 33.7–61.9%, and 88.5–96.6% of the EC, BC,

351 and ACS_{BrC} emissions. The consumption of fireworks showed a trend of inverted U shape. It dominated the
 352 tendencies of EC, BC, and ACS_{BrC} emissions from FMS. Moreover, there was a surge in emissions due to
 353 the high consumption of fireworks in 2014, which is consistent with the temporal distribution of PM_{2.5} (Wei
 354 et al., 2020, 2021) (**Text S6**). The surge in sales might have been caused by destocking after the Air Pollution
 355 Prevention and Control Action Plan (APPCP) was implemented. From 2000 to 2006, the resident's income
 356 raised by 76.5% due to the booming economy. The residents have more money to purchase fireworks. And
 357 only another 12 cities have forbidden fireworks burning in 2000–2006. It can be the reason for the increase
 358 in fireworks consumption amounts. From 2006 to 2018, although people's incomes continued to rise, while
 359 the urbanization rate increased by 16.0% and additional 201 cities have forbidden the fireworks burning,
 360 which lead to the decrease of fireworks consumption amount at this period.



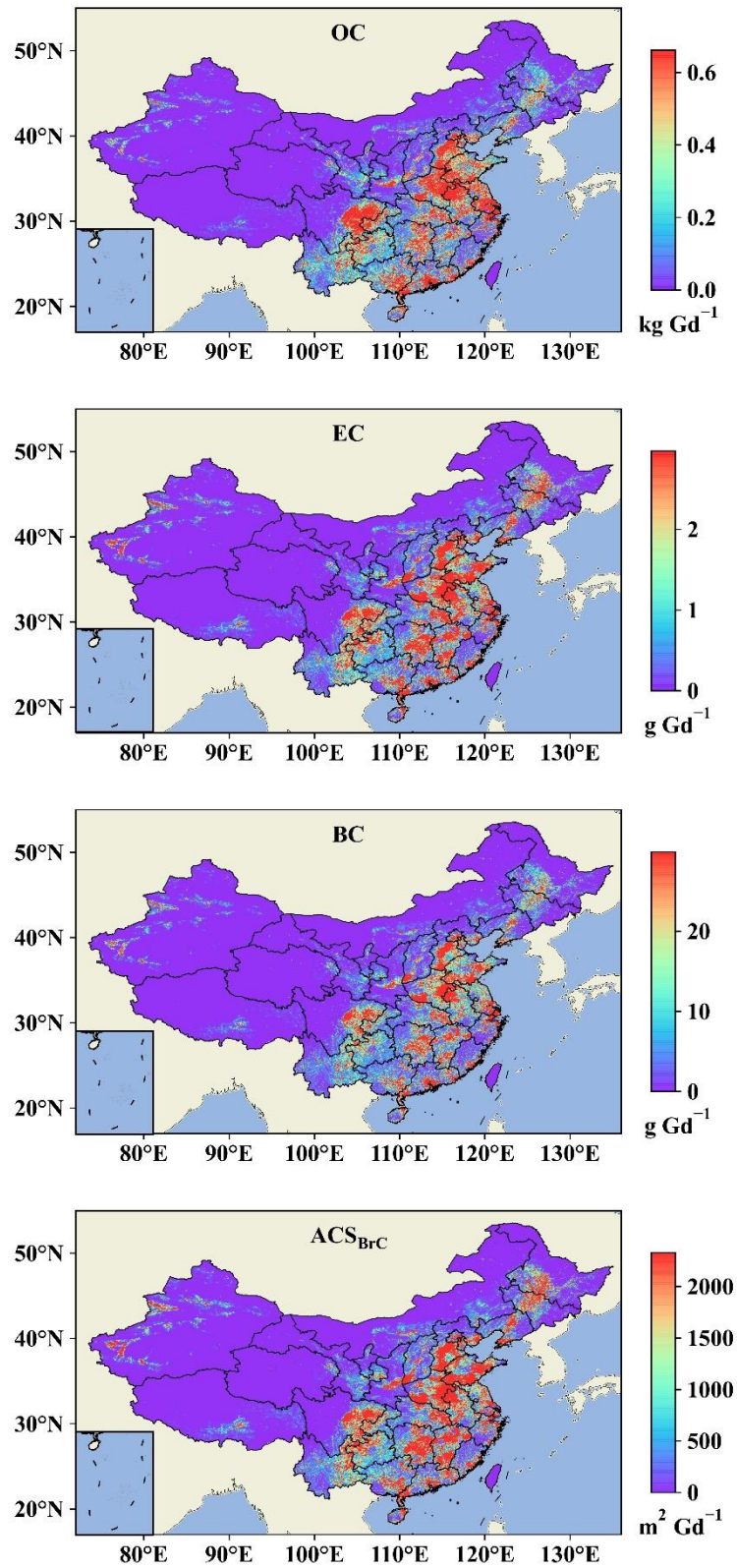
361
 362 **Figure 4** Total CA emission from FMS in China from 2000 to 2018 (SI: sacrificial incense; JP: joss paper; FW: fireworks;
 363 BBQ: barbecue; RC: residential cooking; CI: catering industry).

364 3.3.2 Spatial variation

365 There are seven geographical regions in China (**Figure S9**), of which East China was the largest CA
 366 emission region. East China contributed 24.2–27.7%, 23.9–29.6%, 24.2–29.0%, and 23.5–29.9% of the OC,
 367 EC, BC, and ACS_{BrC} total emissions from FMS, respectively (**Figure 5**). The dense distribution of the
 368 population (28.2–30.3% of the population) was responsible for the high emissions in East China. The OC,

369 EC, and BC emission from FMS in Southernwest China was second to that of East China. OC, EC, and BC
370 emissions in Central China accounted for 21.5–27.2%, 18.0–21.3%, and 19.2–22.5% of their national total
371 emissions. Eating habits in Southernwest China led to its high emission. Southernwest China has a higher
372 density of barbecue restaurants (11.9% higher than the national average) and per capita meat consumption
373 (33.4% higher than the national average), as well as a large population (14.9% of the national total). The
374 ACS_{BrC} emission from Central China was second to that of East China, accounting for 14.3–21.6% of the
375 national total. 90.9–96.4% of ACS_{BrC} emission was from fireworks burning. Hunan province in Central
376 China is one of the main fireworks-producing regions. The density of fireworks stores in Hunan province
377 was 2.3 times that of the national average. What's more, Central China was also one of the densely populated
378 regions, accounting for 16.0–17.6% of the national population. Due to the heating needs in winter, the OC
379 and BC emissions from other sources in North China contributed 14.8–17.2% and 17.6–21.1% of the national
380 total (Li et al., 2017). However, the contributions of OC and BC emissions from FMS in North China were
381 only 7.8–8.5% and 9.5–10.5%. The lower contribution was due to the lower per capita meat consumption
382 (25.4% lower than the national average) and fewer restaurants (5.5% lower than the national average).

383 The emission distributions from different sources showed great differences, which came from the
384 regional culture and economic diversity (**Figure S10** and **Figure S11**). High emission regions of sacrificial
385 incense and joss paper overlapped with the areas with large numbers of temples and cradles of Chinese
386 Buddhism (**Figure S3**, **Text S7**), where people in those areas may be more devout about sacrifice. The
387 distributions of cooking emissions (both residential cooking emissions and catering industry emissions) and
388 barbecue emissions were highly similar to the population distribution, especially in urban regions. This is
389 consistent with previous studies. For example, the cooking-related organic aerosol (COA) concentrations at
390 urban sites (6.46–6.97 $\mu\text{g m}^{-3}$ in Beijing and 14.2 $\mu\text{g m}^{-3}$ in Shijiazhuang) were much higher than that at the
391 rural site (2.96–3.74 $\mu\text{g m}^{-3}$ in Gucheng, a rural site near Beijing), and COA concentration was 0 at the
392 background site (Sun et al., 2013, 2020; Wang et al., 2015b, 2020; Huang et al., 2019). Areas with higher
393 economic consumption have more demands for repast styles and varieties, leading to more emissions.
394 Emissions of fireworks showed an obvious difference in urban and rural regions. Emissions from urban
395 regions were near zero, while emissions from suburbs and rural regions were much higher (more details can
396 be found in **Section 3.3.3**, **Figure 8**).



397
398
399

Figure 5 Spatial distribution of CA emission from FMS in China in 2018. The colorbar showed the emission in each grid.

3.3.3 Intense short-term and regionally concentrated emissions

As shown in **Figure S12** and **Figure S13**, CA emissions from residential sources in winter were extremely higher than in summer resulting from the heating demand (Wang et al., 2012; Huang et al., 2015; Li et al., 2017), while emissions from FMS showed a similar seasonal trend due to the fireworks burning. During the Chinese Spring Festival, fireworks burning results in massive pollutant emissions and severe air pollution (Kong et al., 2015; Yao et al., 2019; Ding et al., 2019; Lai & Brimblecombe, 2020). We have investigated the CA emissions from FMS in the month and at several related Chinese festivals (CNE, CSF, LF, QF, and ZF). As shown in **Figure 6**. The emissions were mostly concentrated in January and February (all CNE and CSF are in the same month in 2000–2018, after the calculation of multi-year data, the results for January and February in **Figure 6** seemed to be lower than those in **Figure S13**). 75.8% of fireworks were set off on CNE and CSF, and 20.4% were set off on LF (**Figure 7**). Thus, the ACS_{BrC} emission on CNE was 1444 times the yearly average, and the OC, EC, and BC emissions were 10.9, 262, and 74.6 times the average, respectively. The highly short-term emission of fireworks led to a sharp increase in the concentration of air pollutants (Vecchi et al., 2008; Shi et al., 2011; Cao et al., 2018; Lai & Brimblecombe, 2020).

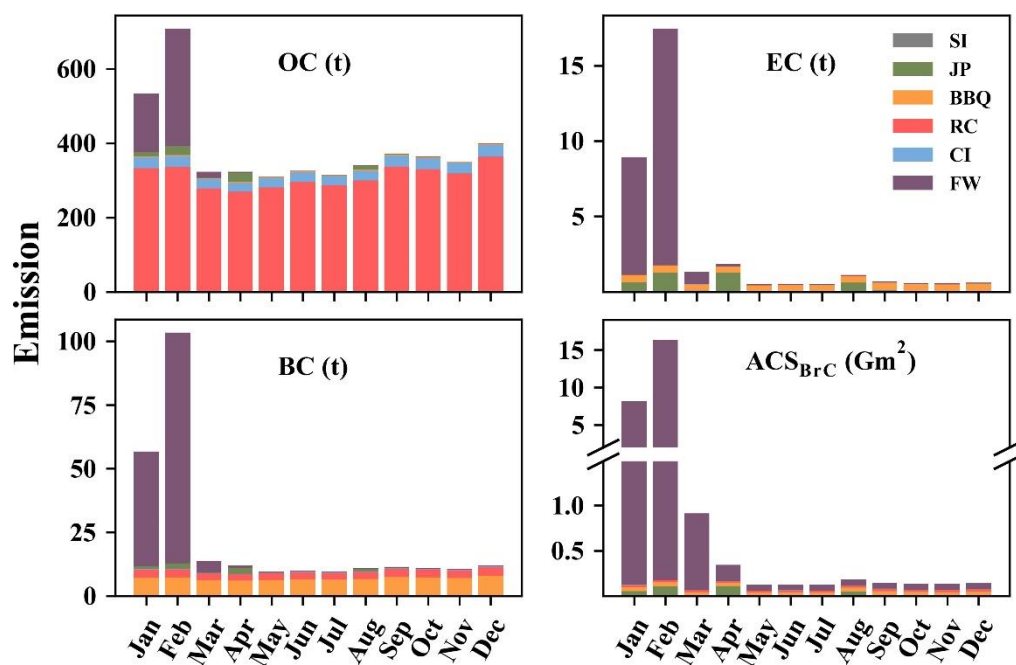
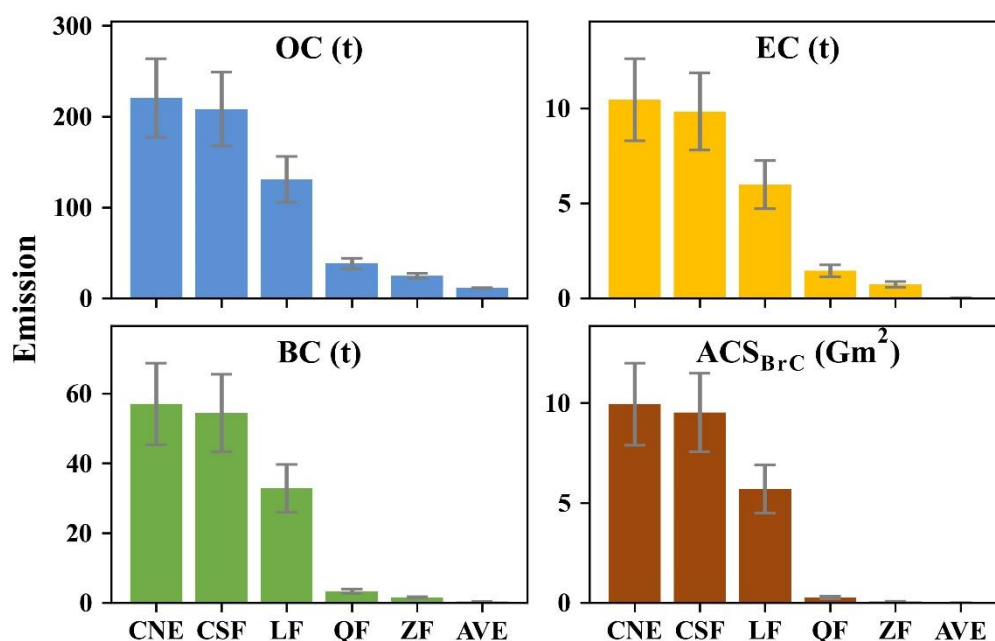


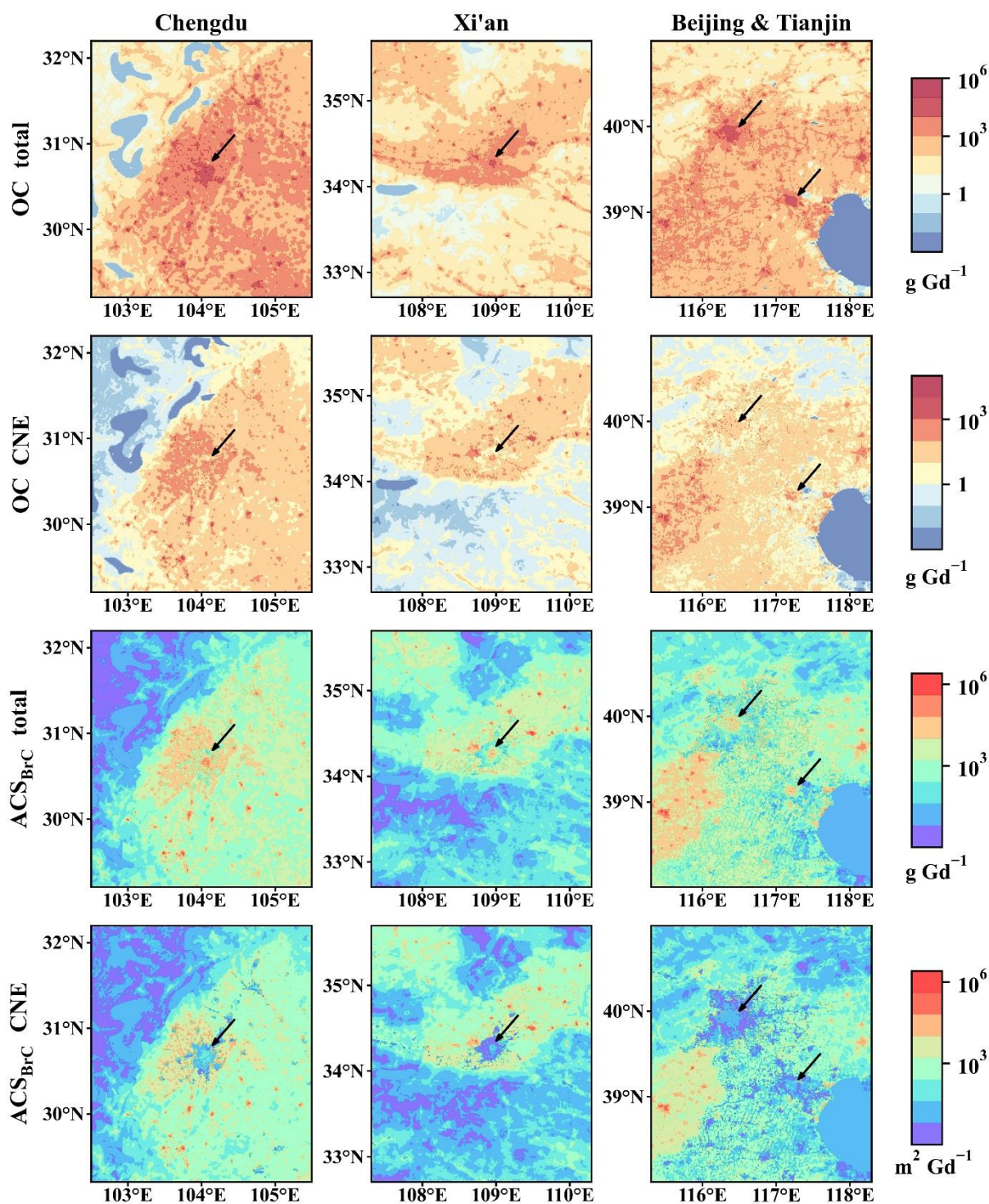
Figure 6 Averaged monthly CA emissions from FMS in China for the year of 2000–2018.



419
 420 **Figure 7** Average CA emissions on Chinese New Year’s Eve (CNE), Chinese Spring Festival (CSF), Spring Lantern Festival
 421 (LF), Qingming Festival (QF), and Zhongyuan Festival (ZF) for the year of 2000–2018. The AVE showed the average daily
 422 emissions except for the festivals mentioned above.

423
 424 For a short-term period, emissions from FMS also showed obvious spatial distribution. 83.2–93.1% of
 425 OC emissions came from barbecue and cooking. The higher population density and living quality led to higher
 426 OC emissions in urban regions. As shown in **Figure 8**, the OC emission intensities (average emission per
 427 grid) in the urban regions of Chengdu, Xi’an, Beijing, and Tianjin were 62.6, 63.1, 27.0, and 14.6 times of
 428 those for rural regions in 2018. This situation was common in China. China set up 13 prevention and control
 429 regions (3 key regions and 10 city clusters, 3-10R) in 2013 to improve air quality, and they are relatively
 430 developed regions (https://www.mee.gov.cn/gkml/hbb/bgg/201303/t20130305_248787.htm). The OC
 431 emission intensities in the urban regions of 3-10R were 3.9–50.5 times those in the surrounding rural regions.
 432 Thus, OC emissions from FMS were concentrated in urban regions overall. Since fireworks burning was
 433 concentrated in CNE or CSF and in rural regions, the feature that OC emission concentrated in urban regions
 434 would be attenuated at CNE. In contrast, ACS_{BrC} emissions tended to concentrate in rural regions, especially
 435 during the periods of CNE and CSF (**Figure 8**). Fireworks burning was the main contributor (>88.5%) to

436 ACS_{BrC} emissions, and the fireworks burning was concentrated in CNE or CSF. The ACS_{BrC} emission
437 intensities in rural regions of Chengdu, Xi'an, Beijing, and Tianjin were 18.8, 20.0, 107, and 150 times those
438 for urban regions at the 2018 CNE. Many cities have introduced policies to control firework burning, and
439 civilized sacrifice is encouraged. But these policies tend to be implemented effectively only in central urban
440 regions. Suburbs and surrounding rural regions, which are densely populated, are areas that policies do not
441 consider or be executed efficiently. The contribution of rural ACS_{BrC} emissions in 3-10R was ~79.0% and
442 even as high as 96.7% at the 2018 CNE. However, the rural population in these regions only accounted for
443 14.1–41.9%. In fact, 63.0–79.5% of ACS_{BrC} emissions at CNE came from the rural regions in China. During
444 the period of CNE and CSF, pollutants emitted from rural residents' activities were likely to be transmitted
445 to urban areas, leading to serious air pollution in urban regions (Yao et al., 2019; Pang et al., 2021).

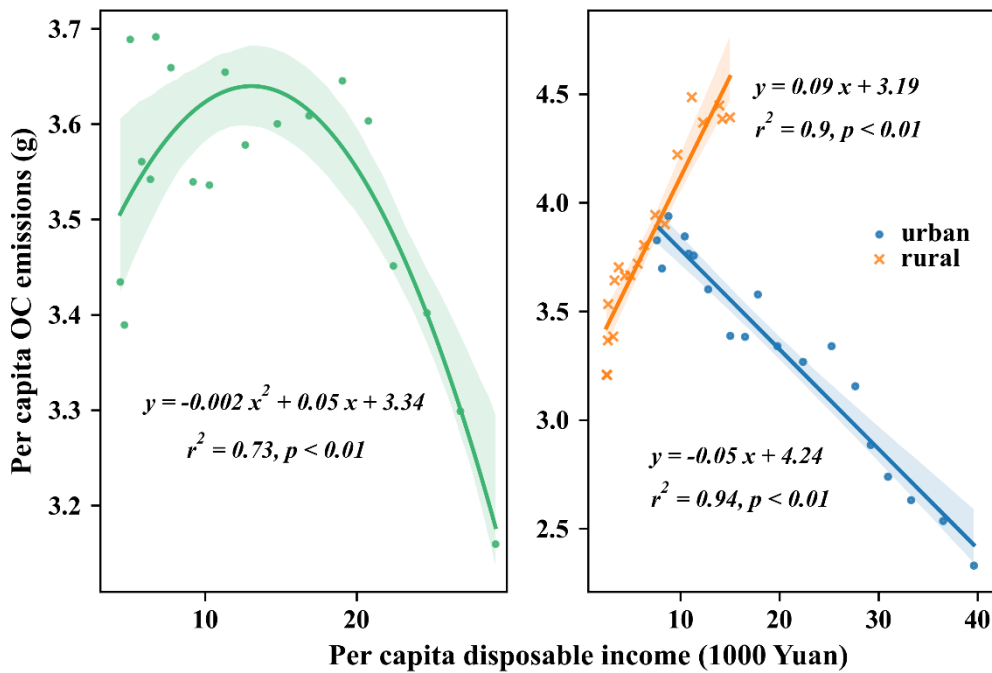


446

447 **Figure 8** Differences in OC (six figures above) and ACS_{BrC} (six figures below) emissions distributions in urban and rural
 448 regions in Chengdu (core city of Sichuan Basin), Xi'an (core city of Guanzhong Plain), and Beijing & Tianjin (Core cities
 449 of North China Plain). The first and second lines showed the total OC emissions in 2018, and in the day of CNE, respectively.
 450 The third and fourth lines showed the ACS_{BrC} emissions in 2018, and in the day of CNE. The arrows pointed to the city
 451 centers. The colorbars showed the emission in each grid for OC and ACS_{BrC}.

3.3.4 Emissions impacted by economical development

Barbecue and cooking contributed a significant portion of OC emissions from FMS, which led to a distinctive feature of emissions from FMS. There was a certain correlation between OC emissions and local economic development. We have gathered disposable income per capita data from 2000 to 2018 for each city. The relationship between the disposable income and OC emission per capita has been assessed. As shown in **Figure 9**, like other emission sources, OC emissions from FMS and disposable income showed an inverted U-shape relationship ($r^2 = 0.73, p < 0.01$) (Environmental Kuznets Curves) (Wu et al., 2020; Zhong et al., 2020). This correlation existed for ACS_{BrC} emissions dominated by fireworks burning, while the correlation was weaker ($r^2 = 0.59, p < 0.01$) than that of OC emissions dominated by cooking sources. If we separated the emission-economical relationship in urban regions from rural regions, the results would be different. The relationships were linear in both urban and rural regions (**Figure 9**). However, the correlation was significantly negative ($r = -0.97, p < 0.01$) in urban regions compared to the positive one ($r = 0.94, p < 0.01$) in rural regions. As discussed above, cooking sources dominated the OC emissions from FMS in China. From 2000 to 2018, meat consumption per capita increased by 83.4%, and the OC emissions per capita have increased by 36.9% in rural regions. In urban regions, meat consumption increased by 22.0%, while OC emissions per capita decreased by 39.1%. The reason for this phenomenon was the higher popularizing rate of range hoods in urban regions, which was 5.2 times that of rural regions. What's more, the popularizing rate of range hoods in urban regions has also increased by 132% in urban regions. As a result, OC emissions that would have been raised were eliminated by a large number of range hoods in urban regions.



471

472 **Figure 9** The relationship between per capita disposable income and OC emissions from FMS for the years of 2000–2018
 473 in China. The left figure showed the invert-U shape relationship between the income and the national average emissions.
 474 The right figure showed the correlation between the income and emissions in urban regions and rural regions. The shaded
 475 areas represent 95% confidence intervals.

476

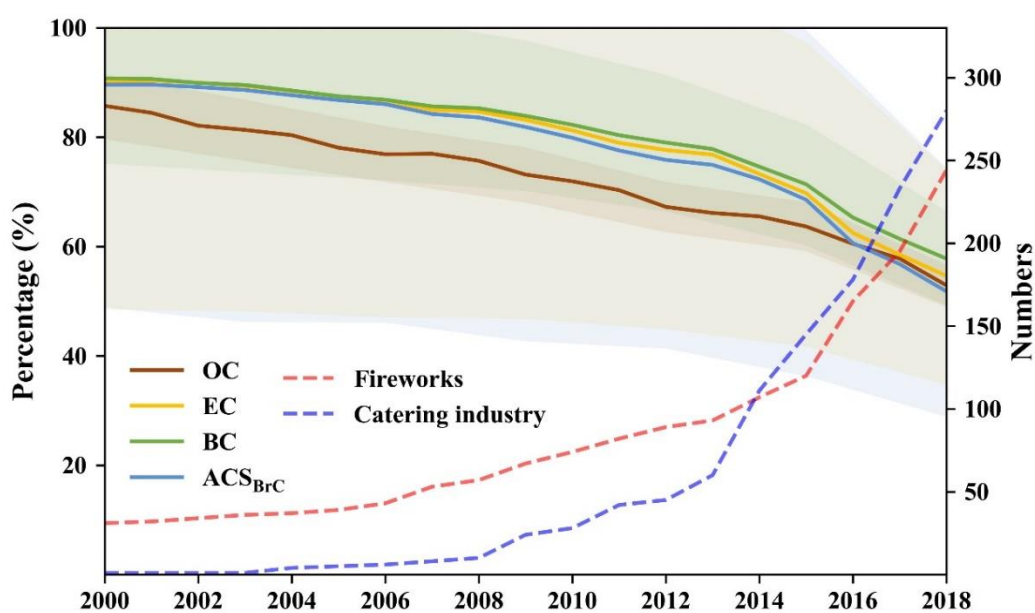
477 In contrast to the relatively developed 3-10R, there are some contiguous poor regions (CPR) in China,
 478 where located in the borderland or mountains (http://www.gov.cn/gzdt/2012-06/14/content_2161045.htm).
 479 The other regions (OR) excluding 3-10R and CPR, were at a moderate level of development in China. The
 480 OC emissions per capita in 3-10R, OR, and CPR, were 3.04–3.77 g, 3.49–4.00 g, and 3.54–4.11 g in 2000–
 481 2018. OC emissions per capita in 3-10R, OR, and CPR have all crossed the inflection point of the emission-
 482 economical correlation. Thus the relatively developed 3-10R have lower per capita emissions. It also verified
 483 the economic impact of OC emissions. However, 3-10R has 76.2–77.4% of the population, thus the emission
 484 intensities in 3-10R were still 3.1–3.4 times that of the national average.

485 3.3.5 The implication for modifying related air pollution control policies

486 To combat air pollution, China introduced its toughest air pollution control plan (APPCP) ever in 2013
 487 (Zhang et al., 2019a). The implementation of the APPCP had led to significant improvements in China's air

488 quality. The control measures of FMS have also begun to be widely promoted (**Figure S14**). There were
 489 76.3% and 66.5% of cities have introduced policies to restrict the emissions from the catering industry and
 490 fireworks burning before 2018. The removal efficiencies of pollutants for small, medium, and large catering
 491 industries were higher than 60%, 75%, and 85% (GB 18483-2001). Local governments have the right to
 492 designate the areas where fireworks were forbidden, usually urban areas, along with hospitals, factories,
 493 power plants, schools, and transportation hubs (http://www.gov.cn/zwgk/2006-01/25/content_170906.htm).
 494 In addition, the government had proposed residents install range hoods to control the emissions from cooking
 495 in APPCP, and the national popularizing rate of range hoods increased by 43.6% from 2000 to 2018. The
 496 control policies and recommendations mentioned above have been implemented at various times in different
 497 cities, and they all have positive significance for emission reduction. As a result, OC, EC, BC, and ACS_{BrC}
 498 emissions from FMS have declined by 14.3–47.1%, 9.8–45.4%, 9.2–42.2%, and 10.4–48.2% in 2000–2018,
 499 respectively (**Figure 10**).

500



501

502 **Figure 10** The impact of policies on the reductions of CA emissions. The solid lines (left y-axis) represented the actual CA
 503 emissions compared to the emissions without the policy impact (100% on the left y-axis). The shaded part of the solid line
 504 represents uncertainties. The dotted line (right y-axis) represented the number of cities that issued policies to control FMS
 505 emissions.

506 If we assume that there was also a quadratic fitting relationship between rural per capita OC emissions
507 and income, then the rural per capita OC emissions would start to decline when rural per capita income
508 reaches 16.8 k Yuan. The control of CA emissions from FMS like cooking should start from the perspective
509 of increasing the income of rural residents. With enough income, residents will tend to a more
510 environmentally friendly and green lifestyle. The green lifestyle is embodied by the installation of a range
511 hood in this work. In 2017, the impervious surfaces of urban regions only accounted for 1.52% of the national
512 area (Gong et al., 2019), and rural regions are vast by contrast. Thus, the cost of controlling the activities of
513 fireworks burning, sacrificial incenses, and joss paper burning in rural regions will be much higher than in
514 urban regions. For these sources, policies and standards should be set to limit their emissions from the
515 burning processes. In addition, it is questionable whether the environmentally friendly fireworks currently
516 on the market have a lower impact on the environment (Fan et al., 2021). Thus, manufacturers should be
517 guided to develop environmentally friendly fireworks, joss paper, and sacrificial incense to reduce emissions.

518 **3.4 Comparison with other studies**

519 As an emission source with less attention, most of the relevant studies focused on the EFs of PM (Jetter
520 et al., 2002; Lee & Wang, 2004; Wang et al., 2015a; Kuo et al., 2016; Jilla & Kura, 2017; Amouei
521 Torkmahalleh et al., 2018; Wang et al., 2018b; Zhao et al., 2018; Lin et al., 2019), PAHs (Yang et al., 2005,
522 2013; Zhao et al., 2019), and VOCs (Cheng et al., 2016; Wang et al., 2018b). Several metallic elements
523 (Croteau et al., 2010; Shen et al., 2017) and organic matters (Xiang et al., 2017; Que et al., 2019) have also
524 been tested. Few studies have tested OC and EC EFs of FMS (See & Balasubramanian, 2011; Zhang et al.,
525 2019b; Lin et al., 2021). Fireworks burning was the least studied emission source, while fireworks can emit
526 large amounts of particles. EFs of PM₁₀ from fireworks burning as 54–429 g kg⁻¹ have been reported
527 (Camilleri & Vella, 2016; Keller & Schragen, 2021), which were much higher than the CA EFs in this study.
528 The EFs in the literatures have been shown in **Table S4**.

529 Several studies have calculated the emission amount of the catering industry (**Table S5**). For example,
530 Wang et al. (2018a) have calculated the VOCs emission (66245 t) from restaurants in China based on
531 samplings of 9 types of restaurants. Jin et al. (2021) have calculated the OC from the catering industry in
532 China by investigations in two cities in Shandong and Shanxi provinces. The results showed that OC
533 emissions from the catering industry were 26.8 Gg, which was 66.0 times that of our results. The EFs used

534 in Jin et al. (2021) were the generation rates of pollutants, which were 0.48 mg m^{-3} for OC in oil fumes.
535 Different EFs and calculation methods may be the main reason for the discrepancy. Emissions from cooking
536 have been reported as the main driver of OC in urban regions, as it contributed large portions of organic
537 aerosols in Shanghai (20–35%) and Beijing (10–19%) (Liu et al., 2021; Zhu et al., 2021b). The effects of
538 cooking emissions on the urban atmosphere should not be neglected when other sources like residential or
539 industry sources were efficiently controlled (Zhang et al., 2021c; Zhu et al., 2021a).

540 Previous research has calculated the total OC and BC emissions in China, such as the widely used MEIC
541 (OC: 2080–3190 Gg, BC: 1253–1728 Gg) and PKU emission inventory (OC: 2345–3587 Gg, BC: 1455–
542 1624 Gg) (Wang et al., 2014a; Huang et al., 2015; Li et al., 2017). Residential sources or residential &
543 commercial source contributed most of OC (80.3% in MEIC, and 71.4% in PKU) and BC (51.5% in MEIC,
544 and 51.0% in PKU) emissions (Peng et al., 2019). The OC and BC emissions from FMS accounted for only
545 1.5–2.2‰ and 0.16–0.20‰ of their national total emission. Thus, the OC and BC emissions from FMS were
546 generally meager. During key periods like the CNE, the contributions of FMS to the total OC and BC
547 emissions can rise to 2.3–3.5% and 1.1–1.6%. In key areas, the contribution rates would be relatively higher.
548 For instance, in CNE of 2014, FMS contributed 6.3% of OC emission in the Sichuan Basin and 2.9% of BC
549 emission in the Jiangxi-Hunan area. However, it should be noted that, the fireworks were always set off from
550 about 20:00 to 00:00 in CNE, so the intensive emission amounts could be considered at these times.
551 Therefore, the contribution of fireworks burning to CA in the atmosphere during CNE and CSF is still open
552 to debate.

553 It has caused widespread controversy that why the governments do not control the emissions from
554 industries and vehicles in CNE but emphasize the control of emissions from fireworks burning. The public
555 can not accept or believe that the emissions from fireworks can lead to serious air pollution, which could be
556 the key reason why they can not be completely eradicated in cities. From this study, the CA emissions are
557 limited compared with those from residential sources. An interesting question that atmospheric scientists
558 needed to be solved in the future is that if the fireworks burning were not controlled, how many air pollutants
559 from other main sources of cities should be controlled alternatively.

560 **Summary and conclusions**

561 The absence of anthropogenic sources in the existing inventory prevents people from drawing accurate

562 conclusions about the control of short-term pollution. To calculate the emissions from these sources which
563 are difficult to estimate, we construct an emission inventory establishment framework including a series of
564 equations and methods. We use multiple proxy data, such as the questionnaire, various statistics, and points
565 of interest, to build a dataset of the activity of five missing sources (FMS, including cooking, fireworks
566 burning, sacrificial incenses, and joss paper burning, and barbecue). The carbonaceous aerosols (CA)
567 emission factors were tested in our lab using a self-designed sampling platform. The OC, EC, and BC EFs
568 varied in 5.86–203 mg kg⁻¹, 0.003–12.4 mg kg⁻¹, and 1.07–191 mg kg⁻¹, respectively. BrC absorption EFs
569 were in the range of 0.01–6.05 m² kg⁻¹ (370 nm). From 2000 to 2018, the activity of FMS emitted 4268–
570 4919 t, 22.6–43.9 t, 213–324 t, and 14.7–35.6 Gm² of OC, EC, BC, and BrC absorption cross-section
571 (ACS_{BrC}, in 370 nm wavelength). Emissions from FMS would concentrate on special festivals. For example,
572 CA emission in Chinses New Year’ eve was more than 10.8 times of its yearly average value. The distribution
573 of pollutants also showed great differences between urban and rural regions due to the demographic,
574 economic, and policy implications. There was a negative correlation ($r = -0.97, p < 0.01$) between individual
575 emissions and disposable income in rural areas and a positive correlation ($r = 0.94, p < 0.01$) in urban areas.
576 The policy implications led to a reduction of over 42.2% of CA emissions from FMS. This study
577 complements the lack of emission inventory research of such missing sources and provides the prerequisite
578 for modeling studies. Meanwhile, we suggest that raising residents’ income can be a feasible solution when
579 reducing FMS emissions sources that are difficult to control. The fireworks burning can be controlled from
580 the manufacturer's side by guiding them to develop more environmentally friendly products. We also suppose
581 that whether it is possible to control other emission sources for providing the environmental capacity for the
582 emissions of fireworks burning.

583 **Data availability**

584 The dataset generated in this work is available at <https://doi.org/10.6084/m9.figshare.19999991.v2>
585 (Cheng et al., 2022). The POI data (points of barbecue restaurants, temples, common restaurants, and
586 firework shops) were from the Open Platform of Amap (<https://lbs.amap.com/>). The China Forestry
587 Statistical Yearbook (forest fires), China Light Industry Yearbook (fireworks export volume), and statistical
588 yearbook of each province (urban and rural population, meat consumption, consumption expenditure, and
589 disposable income) came from <https://data.cnki.net>. The percentage of meals eaten out came from

590 <https://www.chinanutri.cn/>. The China Statistical Yearbook (popularizing rate of the range hood) came from
591 <https://data.cnki.net>. The distribution of population was from www.worldpop.org. The land use data was
592 from <http://data.ess.tsinghua.edu.cn/>. The annual fireworks sales came from
593 <https://www.mem.gov.cn/gk/tjsj/>. The annual and monthly restaurant sales came from
594 <https://data.stats.gov.cn/>.

595 **Author contribution**

596 **Yi Cheng**: Experiments, Visualization, Writing - original draft. **Shaofei Kong**: Conceptualization,
597 Methodology, Supervision, Writing - review & editing. **Liquan Yao**: Experiments, Formal analysis. **Huang**
598 **Zheng**: Experiments, Formal analysis. **Jian Wu**: Formal analysis. **Qin Yan**: Experiments. **Shurui Zheng**:
599 Experiments. **Yao Hu**: Validation, **Zhenzhen Niu**: Experiments. **Yingying Yan**: Supervision. **Zhenxing**
600 **Shen**: Supervision. **Guofeng Shen**: Supervision. **Dantong Liu**: Supervision. **Shuxiao Wang**: Supervision.
601 **Shihua Qi**: Supervision.

602 **Competing interests**

603 The authors declare no competing financial interest.

604 **Acknowledgments**

605 This study was financially supported by the National Natural Science Foundation of China (42077202;
606 41830965), and the Key Program of the Ministry of Science and Technology of the People's Republic of
607 China (2016YFA0602002; 2017YFC0212602).

608

609 **References**

- 610 Amouei Torkmahalleh, M., Ospanova, S., Baibatyrova, A., Nurbay, S., Zhanakhmet, G., & Shah, D. (2018).
611 Contributions of burner, pan, meat and salt to PM emission during grilling. *Environmental Research*,
612 *164*, 11–17. <https://doi.org/10.1016/j.envres.2018.01.044>
- 613 Batis, C., Sotres-Alvarez, D., Gordon-Larsen, P., Mendez, M. A., Adair, L., & Popkin, B. (2014).
614 Longitudinal analysis of dietary patterns in Chinese adults from 1991 to 2009. *British Journal of*
615 *Nutrition*, *111*(8), 1441–1451. <https://doi.org/10.1017/S0007114513003917>
- 616 Bond, T. C., Doherty, S. J., Fahey, D. W., Forster, P. M., Berntsen, T., DeAngelo, B. J., et al. (2013). Bounding
617 the role of black carbon in the climate system: A scientific assessment. *Journal of Geophysical Research:*
618 *Atmospheres*, *118*(11), 5380–5552. <https://doi.org/10.1002/jgrd.50171>
- 619 Camilleri, R., & Vella, A. J. (2016). Emission factors for aerial pyrotechnics and use in assessing
620 environmental impact of firework displays: Case study from Malta. *Propellants, Explosives,*
621 *Pyrotechnics*, *41*(2), 273–280. <https://doi.org/10.1002/prop.201500205>
- 622 Cao, X., Zhang, X., Tong, D. Q., Chen, W., Zhang, S., Zhao, H., & Xiu, A. (2018). Review on
623 physicochemical properties of pollutants released from fireworks: Environmental and health effects and
624 prevention. *Environmental Reviews*, *26*(2), 133–155. <https://doi.org/10.1139/er-2017-0063>
- 625 Chen, Y., Zhi, G., Feng, Y., Liu, D., Zhang, G., Li, J., et al. (2009). Measurements of black and organic
626 carbon emission factors for household coal combustion in China: Implication for emission reduction.
627 *Environmental Science & Technology*, *43*(24), 9495–9500. <https://doi.org/10.1021/es9021766>
- 628 Chen, Y., Tian, C., Feng, Y., Zhi, G., Li, J., & Zhang, G. (2015). Measurements of emission factors of PM_{2.5},
629 OC, EC, and BC for household stoves of coal combustion in China. *Atmospheric Environment*, *109*,
630 190–196. <https://doi.org/10.1016/j.atmosenv.2015.03.023>

- 631 Cheng, S., Wang, G., Lang, J., Wen, W., Wang, X., & Yao, S. (2016). Characterization of volatile organic
632 compounds from different cooking emissions. *Atmospheric Environment*, *145*, 299–307.
633 <https://doi.org/10.1016/j.atmosenv.2016.09.037>
- 634 Cheng, Y., Kong, S., Yan, Q., Liu, H., Wang, W., Chen, K., et al. (2019). Size-segregated emission factors
635 and health risks of PAHs from residential coal flaming/smoldering combustion. *Environmental Science
636 and Pollution Research*, *26*, 31793–31803. <https://doi.org/10.1007/s11356-019-06340-2>
- 637 Cheng, Y., Kong, S., Yao, L., Zheng, H., Wu, J., Yan, Q., et al. (2022). Multi-year emission of carbonaceous
638 aerosols from cooking, fireworks burning, sacrificial incenses, joss paper burning, and barbecue and
639 the key driving forces in China. figshare. Dataset. <https://doi.org/10.6084/m9.figshare.19999991.v2>
- 640 Chiang, K.-C., & Liao, C.-M. (2006). Heavy incense burning in temples promotes exposure risk from
641 airborne PMs and carcinogenic PAHs. *Science of the Total Environment*, *372*(1), 64–75.
642 <https://doi.org/10.1016/j.scitotenv.2006.08.012>
- 643 Corbin, J. C., Pieber, S. M., Czech, H., Zanatta, M., Jakobi, G., Massabò, D., et al. (2018). Brown and black
644 carbon emitted by a marine engine operated on heavy fuel oil and distillate fuels: Optical properties,
645 size distributions, and emission factors. *Journal of Geophysical Research: Atmospheres*, *123*(11), 6175–
646 6195. <https://doi.org/10.1029/2017JD027818>
- 647 Croteau, G., Dills, R., Beaudreau, M., & Davis, M. (2010). Emission factors and exposures from ground-
648 level pyrotechnics. *Atmospheric Environment*, *44*(27), 3295–3303.
649 <https://doi.org/10.1016/j.atmosenv.2010.05.048>
- 650 Ding, J., Guo, J., Wang, L., Chen, Y., Hu, B., Li, Y., et al. (2019). Cellular responses to exposure to outdoor
651 air from the Chinese Spring Festival at the air–liquid interface. *Environmental Science & Technology*,

652 53(15), 9128–9138. <https://doi.org/10.1021/acs.est.9b00399>

653 Ding, Q., Liu, J., Lu, Y., Wang, Y., Lu, F., & Shi, J. (2014). Research and development of an on-line
654 carbonaceous aerosol analyzer (In Chinese). *Chinese Journal of Scientific Instrument*, 35(06), 1246–
655 1253. <https://doi.org/10.19650/j.cnki.cjsi.2014.06.007>

656 Drinovec, L., Močnik, G., Zotter, P., Prévôt, A. S. H., Ruckstuhl, C., Coz, E., et al. (2015). The “dual-spot”
657 Aethalometer: An improved measurement of aerosol black carbon with real-time loading compensation.
658 *Atmospheric Measurement Techniques*, 8(5), 1965–1979. <https://doi.org/10.5194/amt-8-1965-2015>

659 Fan, S., Li, Y., & Liu, C. (2021). Are environmentally friendly fireworks really “green” for air quality? A
660 study from the 2019 National Day fireworks display in Shenzhen. *Environmental Science & Technology*,
661 55(6), 3520–3529. <https://doi.org/10.1021/acs.est.0c03521>

662 Feng, Y., Ramanathan, V., & Kotamarthi, V. R. (2013). Brown carbon: A significant atmospheric absorber of
663 solar radiation? *Atmospheric Chemistry and Physics*, 13(17), 8607–8621. [https://doi.org/10.5194/acp-](https://doi.org/10.5194/acp-13-8607-2013)
664 13-8607-2013

665 Gong, P., Li, X., & Zhang, W. (2019). 40-Year (1978–2017) human settlement changes in China reflected by
666 impervious surfaces from satellite remote sensing. *Science Bulletin*, 64(11), 756–763.
667 <https://doi.org/10.1016/j.scib.2019.04.024>

668 Gong, P., Chen, B., Li, X., Liu, H., Wang, J., Bai, Y., et al. (2020). Mapping essential urban land use
669 categories in China (EULUC-China): Preliminary results for 2018. *Science Bulletin*, 65(3), 182–187.
670 <https://doi.org/10.1016/j.scib.2019.12.007>

671 Ho, C.-C., Chan, C.-C., Chio, C.-P., Lai, Y.-C., Chang-Chien, G.-P., Chow, J. C., et al. (2016). Source
672 apportionment of mass concentration and inhalation risk with long-term ambient PCDD/Fs

673 measurements in an urban area. *Journal of Hazardous Materials*, 317, 180–187.
674 <https://doi.org/10.1016/j.jhazmat.2016.05.059>

675 Hu, R., Wang, S., Zheng, H., Zhao, B., Liang, C., Chang, X., et al. (2021). Variations and sources of organic
676 aerosol in winter Beijing under markedly reduced anthropogenic activities during COVID-2019.
677 *Environmental Science & Technology*, acs.est.1c05125. <https://doi.org/10.1021/acs.est.1c05125>

678 Huang, D. D., Zhu, S., An, J., Wang, Q., Qiao, L., Zhou, M., et al. (2021). Comparative assessment of
679 cooking emission contributions to urban organic aerosol using online molecular tracers and Aerosol
680 Mass Spectrometry measurements. *Environmental Science & Technology*, 55(21), 14526–14535.
681 <https://doi.org/10.1021/acs.est.1c03280>

682 Huang, R.-J., Wang, Y., Cao, J., Lin, C., Duan, J., Chen, Q., et al. (2019). Primary emissions versus secondary
683 formation of fine particulate matter in the most polluted city (Shijiazhuang) in North China.
684 *Atmospheric Chemistry and Physics*, 19(4), 2283–2298. <https://doi.org/10.5194/acp-19-2283-2019>

685 Huang, Y., Shen, H., Chen, Y., Zhong, Q., Chen, H., Wang, R., et al. (2015). Global organic carbon emissions
686 from primary sources from 1960 to 2009. *Atmospheric Environment*, 122, 505–512.
687 <https://doi.org/10.1016/j.atmosenv.2015.10.017>

688 Janssens-Maenhout, G., Crippa, M., Guizzardi, D., Muntean, M., Schaaf, E., Dentener, F., et al. (2019).
689 EDGAR v4.3.2 Global Atlas of the three major greenhouse gas emissions for the period 1970-2012.
690 *Earth System Science Data*, 11(3), 959–1002. <https://doi.org/10.5194/essd-11-959-2019>

691 Jetter, J. J., Guo, Z., McBrien, J. A., & Flynn, M. R. (2002). Characterization of emissions from burning
692 incense. *Science of the Total Environment*, 295(1–3), 51–67. [https://doi.org/10.1016/S0048-](https://doi.org/10.1016/S0048-9697(02)00043-8)
693 [9697\(02\)00043-8](https://doi.org/10.1016/S0048-9697(02)00043-8)

694 Jilla, A., & Kura, B. (2017). Particulate matter and carbon monoxide emission factors from incense burning.
695 *Environment Pollution and Climate Change*, 01(04). <https://doi.org/10.4172/2573-458X.1000140>

696 Jin, W., Zhi, G., Zhang, Y., Wang, L., Guo, S., Zhang, Y., et al. (2021). Toward a national emission inventory
697 for the catering industry in China. *Science of the Total Environment*, 754, 142184.
698 <https://doi.org/10.1016/j.scitotenv.2020.142184>

699 Keller, F., & Schragen, C. (2021). Determination of particulate matter emission factors of common
700 pyrotechnic articles. *Propellants, Explosives, Pyrotechnics*, 46(5), 825–842.
701 <https://doi.org/10.1002/prep.202000292>

702 Kong, S. F., Li, L., Li, X. X., Yin, Y., Chen, K., Liu, D. T., et al. (2015). The impacts of firework burning at
703 the Chinese Spring Festival on air quality: Insights of tracers, source evolution and aging processes.
704 *Atmospheric Chemistry and Physics*, 15(4), 2167–2184. <https://doi.org/10.5194/acp-15-2167-2015>

705 Kuo, S.-C., Tsai, Y. I., & Sopajaree, K. (2016). Emission characteristics of carboxylates in PM_{2.5} from
706 incense burning with the effect of light on acetate. *Atmospheric Environment*, 138, 125–134.
707 <https://doi.org/10.1016/j.atmosenv.2016.05.004>

708 Lai, Y., & Brimblecombe, P. (2020). Changes in air pollution and attitude to fireworks in Beijing.
709 *Atmospheric Environment*, 231, 117549. <https://doi.org/10.1016/j.atmosenv.2020.117549>

710 Lao, J.-Y., Xie, S.-Y., Wu, C.-C., Bao, L.-J., Tao, S., & Zeng, E. Y. (2018). Importance of dermal absorption
711 of polycyclic aromatic hydrocarbons derived from barbecue fumes. *Environmental Science &
712 Technology*, 52(15), 8330–8338. <https://doi.org/10.1021/acs.est.8b01689>

713 Laskin, A., Laskin, J., & Nizkorodov, S. A. (2015). Chemistry of atmospheric brown carbon. *Chemical
714 Reviews*, 115(10), 4335–4382. <https://doi.org/10.1021/cr5006167>

- 715 Lee, S.-C., & Wang, B. (2004). Characteristics of emissions of air pollutants from burning of incense in a
716 large environmental chamber. *Atmospheric Environment*, 38(7), 941–951.
717 <https://doi.org/10.1016/j.atmosenv.2003.11.002>
- 718 Li, M., Liu, H., Geng, G., Hong, C., Liu, F., Song, Y., et al. (2017). Anthropogenic emission inventories in
719 China: a review. *National Science Review*, 4(6), 834–866. <https://doi.org/10.1093/nsr/nwx150>
- 720 Liakakou, E., Kaskaoutis, D. G., Grivas, G., Stavroulas, I., Tsagkaraki, D., Paraskevopoulou, D., et al. (2020).
721 Long-term brown carbon spectral characteristics in a Mediterranean city (Athens). *Science of the Total*
722 *Environment*, 708, 135019. <https://doi.org/10.1016/j.scitotenv.2019.135019>
- 723 Lin, M.-D., Rau, J.-Y., Tseng, H.-H., Wey, M.-Y., Chu, C.-W., Lin, Y.-H., et al. (2008). Characterizing PAH
724 emission concentrations in ambient air during a large-scale joss paper open-burning event. *Journal of*
725 *Hazardous Materials*, 156(1–3), 223–229. <https://doi.org/10.1016/j.jhazmat.2007.12.015>
- 726 Lin, P., He, W., Nie, L., Schauer, J. J., Wang, Y., Yang, S., & Zhang, Y. (2019). Comparison of PM_{2.5} emission
727 rates and source profiles for traditional Chinese cooking styles. *Environmental Science and Pollution*
728 *Research*, 26, 21239–21252. <https://doi.org/10.1007/s11356-019-05193-z>
- 729 Lin, P., Gao, J., He, W., Nie, L., Schauer, J. J., Yang, S., et al. (2021). Estimation of commercial cooking
730 emissions in real-world operation: Particulate and gaseous emission factors, activity influencing and
731 modelling. *Environmental Pollution*, 289, 117847. <https://doi.org/10.1016/j.envpol.2021.117847>
- 732 Liu, J., Zhang, F., Xu, W., Chen, L., Ren, J., Jiang, S., et al. (2021). A large impact of cooking organic aerosol
733 (COA) on particle hygroscopicity and CCN activity in urban atmosphere. *Journal of Geophysical*
734 *Research: Atmospheres*, 126(8). <https://doi.org/10.1029/2020JD033628>
- 735 Liu, Z., Guan, D., Wei, W., Davis, S. J., Ciais, P., Bai, J., et al. (2015). Reduced carbon emission estimates

736 from fossil fuel combustion and cement production in China. *Nature*, 524(7565), 335–338.
737 <https://doi.org/10.1038/nature14677>

738 Lui, K. H., Bandowe, B. A. M., Ho, S. S. H., Chuang, H.-C., Cao, J.-J., Chuang, K.-J., et al. (2016).
739 Characterization of chemical components and bioreactivity of fine particulate matter (PM_{2.5}) during
740 incense burning. *Environmental Pollution*, 213, 524–532. <https://doi.org/10.1016/j.envpol.2016.02.053>

741 Martinsson, J., Eriksson, A. C., Nielsen, I. E., Malmborg, V. B., Ahlberg, E., Andersen, C., & Lindgren, R.
742 (2015). Impacts of combustion conditions and photochemical processing on the light absorption of
743 biomass combustion aerosol. *Environmental Science & Technology*, 49, 14663–14671.
744 <https://doi.org/10.1021/acs.est.5b03205>

745 McDuffie, E. E., Smith, S. J., O'Rourke, P., Tibrewal, K., Venkataraman, C., Marais, E. A., et al. (2020). A
746 global anthropogenic emission inventory of atmospheric pollutants from sector- and fuel-specific
747 sources (1970–2017): An application of the Community Emissions Data System (CEDS). *Earth System
748 Science Data*, 12(4), 3413–3442. <https://doi.org/10.5194/essd-12-3413-2020>

749 Meng, W., Zhong, Q., Chen, Y., Shen, H., Yun, X., Smith, K. R., et al. (2019). Energy and air pollution
750 benefits of household fuel policies in northern China. *Proceedings of the National Academy of Sciences*,
751 116(34), 16773–16780. <https://doi.org/10.1073/pnas.1904182116>

752 Pang, N., Gao, J., Zhao, P., Wang, Y., Xu, Z., & Chai, F. (2021). The impact of fireworks control on air
753 quality in four Northern Chinese cities during the Spring Festival. *Atmospheric Environment*, 244,
754 117958. <https://doi.org/10.1016/j.atmosenv.2020.117958>

755 Park, R. J., Kim, M. J., Jeong, J. I., Youn, D., & Kim, S. (2010). A contribution of brown carbon aerosol to
756 the aerosol light absorption and its radiative forcing in East Asia. *Atmospheric Environment*, 44(11),

757 1414–1421. <https://doi.org/10.1016/j.atmosenv.2010.01.042>

758 Peng, L., Zhang, Q., Yao, Z., Mauzerall, D. L., Kang, S., Du, Z., et al. (2019). Underreported coal in statistics:
759 A survey-based solid fuel consumption and emission inventory for the rural residential sector in China.
760 *Applied Energy*, 235, 1169–1182. <https://doi.org/10.1016/j.apenergy.2018.11.043>

761 Que, D. E., Hou, W.-C., Lin, S.-L., Tsai, Y.-I., Lu, I.-C., Wang, L.-C., et al. (2019). Emission of carbonyl
762 compounds from cooking oil fumes in the night market areas. *Aerosol and Air Quality Research*, 19(7),
763 1566–1578. <https://doi.org/10.4209/aaqr.2019.06.0289>

764 Ramanathan, V., & Carmichael, G. (2008). Global and regional climate changes due to black carbon. *Nature*
765 *Geoscience*, 1(4), 221–227. <https://doi.org/10.1038/ngeo156>

766 Saito, E., Tanaka, N., Miyazaki, A., & Tsuzaki, M. (2014). Concentration and particle size distribution of
767 polycyclic aromatic hydrocarbons formed by thermal cooking. *Food Chemistry*, 153, 285–291.
768 <https://doi.org/10.1016/j.foodchem.2013.12.055>

769 Saleh, R., Hennigan, C. J., McMeeking, G. R., Chuang, W. K., Robinson, E. S., Coe, H., et al. (2013).
770 Absorptivity of brown carbon in fresh and photo-chemically aged biomass-burning emissions.
771 *Atmospheric Chemistry and Physics*, 13(15), 7683–7693. <https://doi.org/10.5194/acp-13-7683-2013>

772 See, S. W., & Balasubramanian, R. (2011). Characterization of fine particle emissions from incense burning.
773 *Building and Environment*, 46, 1074–1080. <https://doi.org/10.1016/j.buildenv.2010.11.006>

774 Shen, G., Xue, M., Chen, Y., Yang, C., Li, W., Shen, H., et al. (2014). Comparison of carbonaceous particulate
775 matter emission factors among different solid fuels burned in residential stoves. *Atmospheric*
776 *Environment*, 89, 337–345. <https://doi.org/10.1016/j.atmosenv.2014.01.033>

777 Shen, H., Tsai, C.-M., Yuan, C.-S., Jen, Y.-H., & Ie, I.-R. (2017). How incense and joss paper burning during

778 the worship activities influences ambient mercury concentrations in indoor and outdoor environments
779 of an Asian temple? *Chemosphere*, 167, 530–540. <https://doi.org/10.1016/j.chemosphere.2016.09.159>

780 Shi, Y., Zhang, N., Gao, J., Li, X., & Cai, Y. (2011). Effect of fireworks display on perchlorate in air aerosols
781 during the Spring Festival. *Atmospheric Environment*, 45(6), 1323–1327.
782 <https://doi.org/10.1016/j.atmosenv.2010.11.056>

783 Sun, J., Zhi, G., Hitzenberger, R., Chen, Y., Tian, C., Zhang, Y., et al. (2017). Emission factors and light
784 absorption properties of brown carbon from household coal combustion in China. *Atmospheric*
785 *Chemistry and Physics*, 17(7), 4769–4780. <https://doi.org/10.5194/acp-17-4769-2017>

786 Sun, Y., He, Y., Kuang, Y., Xu, W., Song, S., Ma, N., et al. (2020). Chemical differences between PM₁ and
787 PM_{2.5} in highly polluted environment and implications in air pollution studies. *Geophysical Research*
788 *Letters*, 47(5). <https://doi.org/10.1029/2019GL086288>

789 Sun, Y. L., Wang, Z. F., Fu, P. Q., Yang, T., Jiang, Q., Dong, H. B., et al. (2013). Aerosol composition, sources
790 and processes during wintertime in Beijing, China. *Atmospheric Chemistry and Physics*, 13(9), 4577–
791 4592. <https://doi.org/10.5194/acp-13-4577-2013>

792 Tanda, S., Licbinsky, R., Hegrova, J., & Goessler, W. (2019). Impact of New Year’s Eve fireworks on the
793 size resolved element distributions in airborne particles. *Environment International*, 128, 371–378.
794 <https://doi.org/10.1016/j.envint.2019.04.071>

795 Tian, J., Wang, Q., Ni, H., Wang, M., Zhou, Y., Han, Y., et al. (2019). Emission characteristics of primary
796 brown carbon absorption from biomass and coal burning: Development of an optical emission inventory
797 for China. *Journal of Geophysical Research: Atmospheres*, 124, 1879–1893.
798 <https://doi.org/10.1029/2018JD029352>

- 799 Tong, D., Cheng, J., Liu, Y., Yu, S., Yan, L., Hong, C., et al. (2020). Dynamic projection of anthropogenic
800 emissions in China: Methodology and 2015–2050 emission pathways under a range of socio-economic,
801 climate policy, and pollution control scenarios. *Atmospheric Chemistry and Physics*, 20, 5729–5757.
802 <https://doi.org/10.5194/acp-20-5729-2020>
- 803 Vecchi, R., Bernardoni, V., Cricchio, D., D’Alessandro, A., Fermo, P., Lucarelli, F., et al. (2008). The impact
804 of fireworks on airborne particles. *Atmospheric Environment*, 42(6), 1121–1132.
- 805 Venkataraman, C., Habib, G., Eiguren-Fernandez, A., Miguel, A. H., & Friedlander, S. K. (2005). Residential
806 biofuels in South Asia: Carbonaceous aerosol emissions and climate impacts. *Science*, 307(5714),
807 1454–1456. <https://doi.org/10.1126/science.1104359>
- 808 Wang, G., Cheng, S., Wei, W., Wen, W., Wang, X., & Yao, S. (2015a). Chemical characteristics of fine
809 particles emitted from different Chinese cooking styles. *Aerosol and Air Quality Research*, 15(6), 2357–
810 2366. <https://doi.org/10.4209/aaqr.2015.02.0079>
- 811 Wang, H., Xiang, Z., Wang, L., Jing, S., Lou, S., Tao, S., et al. (2018a). Emissions of volatile organic
812 compounds (VOCs) from cooking and their speciation: A case study for Shanghai with implications for
813 China. *Science of the Total Environment*, 621, 1300–1309.
814 <https://doi.org/10.1016/j.scitotenv.2017.10.098>
- 815 Wang, L., Xiang, Z., Stevanovic, S., Ristovski, Z., Salimi, F., Gao, J., et al. (2017). Role of Chinese cooking
816 emissions on ambient air quality and human health. *Science of the Total Environment*, 589, 173–181.
817 <https://doi.org/10.1016/j.scitotenv.2017.02.124>
- 818 Wang, L., Zheng, X., Stevanovic, S., Wu, X., Xiang, Z., Yu, M., & Liu, J. (2018b). Characterization
819 particulate matter from several Chinese cooking dishes and implications in health effects. *Journal of*

820 *Environmental Sciences*, 72, 98–106. <https://doi.org/10.1016/j.jes.2017.12.015>

821 Wang, Q., Sun, Y., Jiang, Q., Du, W., Sun, C., Fu, P., & Wang, Z. (2015b). Chemical composition of aerosol
822 particles and light extinction apportionment before and during the heating season in Beijing, China.
823 *Journal of Geophysical Research: Atmospheres*, 120(24), 12708–12722.
824 <https://doi.org/10.1002/2015JD023871>

825 Wang, R., Tao, S., Wang, W., Liu, J., Shen, H., Shen, G., et al. (2012). Black carbon emissions in China from
826 1949 to 2050. *Environmental Science & Technology*, 46(14), 7595–7603.
827 <https://doi.org/10.1021/es3003684>

828 Wang, R., Tao, S., Shen, H., Huang, Y., Chen, H., Balkanski, Y., et al. (2014a). Trend in global black carbon
829 emissions from 1960 to 2007. *Environmental Science & Technology*, 48(12), 6780–6787.
830 <https://doi.org/10.1021/es5021422>

831 Wang, X., Heald, C. L., Ridley, D. A., Schwarz, J. P., Spackman, J. R., Perring, A. E., et al. (2014b).
832 Exploiting simultaneous observational constraints on mass and absorption to estimate the global direct
833 radiative forcing of black carbon and brown carbon. *Atmospheric Chemistry and Physics*, 14(20),
834 10989–11010. <https://doi.org/10.5194/acp-14-10989-2014>

835 Wang, Y., Wang, Q., Ye, J., Li, L., Zhou, J., Ran, W., et al. (2020). Chemical composition and sources of
836 submicron aerosols in winter at a regional site in Beijing-Tianjin-Hebei region: Implications for the
837 Joint Action Plan. *Science of The Total Environment*, 719, 137547.
838 <https://doi.org/10.1016/j.scitotenv.2020.137547>

839 Wei, J., Li, Z., Cribb, M., Huang, W., Xue, W., Sun, L., et al. (2020). Improved 1 km resolution PM_{2.5}
840 estimates across China using enhanced space–time extremely randomized trees. *Atmospheric Chemistry*

841 *and Physics*, 20(6), 3273–3289. <https://doi.org/10.5194/acp-20-3273-2020>

842 Wei, J., Li, Z., Lyapustin, A., Sun, L., Peng, Y., Xue, W., et al. (2021). Reconstructing 1-km-resolution high-
843 quality PM_{2.5} data records from 2000 to 2018 in China: spatiotemporal variations and policy
844 implications. *Remote Sensing of Environment*, 252, 112136. <https://doi.org/10.1016/j.rse.2020.112136>

845 Wu, C., Bao, L., Guo, Y., Li, S., & Zeng, E. Y. (2015). Barbecue fumes: An overlooked source of health
846 hazards in outdoor settings. *Environmental Science & Technology*, 49(17), 10607–10615.
847 <https://doi.org/10.1021/acs.est.5b01494>

848 Wu, J., Kong, S., Wu, F., Cheng, Y., Zheng, S., Yan, Q., et al. (2018). Estimating the open biomass burning
849 emissions in central and eastern China from 2003 to 2015 based on satellite observation. *Atmospheric
850 Chemistry and Physics*, 18, 11623–11646. <https://doi.org/10.5194/acp-18-11623-2018>

851 Wu, J., Kong, S., Zeng, X., Cheng, Y., Yan, Q., Zheng, H., et al. (2021). First high-resolution emission
852 inventory of levoglucosan for biomass burning and non-biomass burning sources in China.
853 *Environmental Science & Technology*, 55(3), 1497–1507. <https://doi.org/10.1021/acs.est.0c06675>

854 Xiang, Z., Wang, H., Stevanovic, S., Jing, S., Lou, S., Tao, S., et al. (2017). Assessing impacts of factors on
855 carbonyl compounds emissions produced from several typical Chinese cooking. *Building and
856 Environment*, 125, 348–355. <https://doi.org/10.1016/j.buildenv.2017.08.045>

857 Xu M., Chao X., Zhang B., Liu S., Yin J., & Gan S. (2018). Study on the investigation, analysis and
858 countermeasures for the current status of mutton sheep industry in Xinjiang (In Chinese). *Acta
859 Ecologiae Animalis Domastici*, 39(3), 85–89.

860 Yan, Q., Kong, S., Yan, Y., Liu, H., Wang, W., Chen, K., et al. (2020). Emission and simulation of primary
861 fine and submicron particles and water-soluble ions from domestic coal combustion in China.

- 862 *Atmospheric Environment*, 224, 117308. <https://doi.org/10.1016/j.atmosenv.2020.117308>
- 863 Yang, C.-R., Ko, T.-H., Lin, Y.-C., Lee, S.-Z., Chang, Y.-F., & Hsueh, H.-T. (2013). Oyster shell reduces
864 PAHs and particulate matter from incense burning. *Environmental Chemistry Letters*, 11(1), 33–40.
865 <https://doi.org/10.1007/s10311-012-0374-2>
- 866 Yang, H.-H., Jung, R.-C., Wang, Y.-F., & Hsieh, L.-T. (2005). Polycyclic aromatic hydrocarbon emissions
867 from joss paper furnaces. *Atmospheric Environment*, 39(18), 3305–3312.
868 <https://doi.org/10.1016/j.atmosenv.2005.01.052>
- 869 Yao, L., Wang, D., Fu, Q., Qiao, L., Wang, H., Li, L., et al. (2019). The effects of firework regulation on air
870 quality and public health during the Chinese Spring Festival from 2013 to 2017 in a Chinese megacity.
871 *Environment International*, 126, 96–106. <https://doi.org/10.1016/j.envint.2019.01.037>
- 872 Zhang, A., Wang, Y., Zhang, Y., Weber, R. J., Song, Y., Ke, Z., & Zou, Y. (2020a). Modeling the global
873 radiative effect of brown carbon: A potentially larger heating source in the tropical free troposphere
874 than black carbon. *Atmospheric Chemistry and Physics*, 20(4), 1901–1920. [https://doi.org/10.5194/acp-](https://doi.org/10.5194/acp-20-1901-2020)
875 [20-1901-2020](https://doi.org/10.5194/acp-20-1901-2020)
- 876 Zhang, L., Gao, Y., Wu, S., Zhang, S., Smith, K. R., Yao, X., & Gao, H. (2020b). Global impact of
877 atmospheric arsenic on health risk: 2005 to 2015. *Proceedings of the National Academy of Sciences*,
878 117(25), 13975–13982. <https://doi.org/10.1073/pnas.2002580117>
- 879 Zhang, L., Luo, Z., Du, W., Li, G., Shen, G., Cheng, H., & Tao, S. (2020c). Light absorption properties and
880 absorption emission factors for indoor biomass burning. *Environmental Pollution*, 267, 115652.
881 <https://doi.org/10.1016/j.envpol.2020.115652>
- 882 Zhang, L., Luo, Z., Li, Y., Chen, Y., Du, W., Li, G., et al. (2021a). Optically measured black and particulate

883 brown carbon emission factors from real-world residential combustion predominantly affected by fuel
884 differences. *Environmental Science & Technology*, 55(1), 169–178.
885 <https://doi.org/10.1021/acs.est.0c04784>

886 Zhang, Q., Zheng, Y., Tong, D., Shao, M., Wang, S., Zhang, Y., et al. (2019a). Drivers of improved PM_{2.5} air
887 quality in China from 2013 to 2017. *Proceedings of the National Academy of Sciences*, 116(49), 24463–
888 24469. <https://doi.org/10.1073/pnas.1907956116>

889 Zhang, S., Zhong, L., Chen, X., Liu, Y., Zhai, X., Xue, Y., et al. (2019b). Emissions characteristics of
890 hazardous air pollutants from the incineration of sacrificial offerings. *Atmosphere*, 10(6), 332.
891 <https://doi.org/10.3390/atmos10060332>

892 Zhang, Y., Kong, S., Sheng, J., Zhao, D., Ding, D., Yao, L., et al. (2021b). Real-time emission and stage-
893 dependent emission factors/ratios of specific volatile organic compounds from residential biomass
894 combustion in China. *Atmospheric Research*, 248, 105189.
895 <https://doi.org/10.1016/j.atmosres.2020.105189>

896 Zhang, Z., Zhu, W., Hu, M., Liu, K., Wang, H., Tang, R., et al. (2021c). Formation and evolution of secondary
897 organic aerosols derived from urban-lifestyle sources: Vehicle exhaust and cooking emissions.
898 *Atmospheric Chemistry and Physics*, 21(19), 15221–15237. [https://doi.org/10.5194/acp-21-15221-](https://doi.org/10.5194/acp-21-15221-2021)
899 2021

900 Zhao, Y., Chen, C., & Zhao, B. (2018). Is oil temperature a key factor influencing air pollutant emissions
901 from Chinese cooking? *Atmospheric Environment*, 193, 190–197.
902 <https://doi.org/10.1016/j.atmosenv.2018.09.012>

903 Zhao, Y., Chen, C., & Zhao, B. (2019). Emission characteristics of PM_{2.5}-bound chemicals from residential

904 Chinese cooking. *Building and Environment*, 149, 623–629.
905 <https://doi.org/10.1016/j.buildenv.2018.12.060>

906 Zheng, B., Tong, D., Li, M., Liu, F., Hong, C., Geng, G., et al. (2018). Trends in China’s anthropogenic
907 emissions since 2010 as the consequence of clean air actions. *Atmospheric Chemistry and Physics*, 18,
908 14095–14111. <https://doi.org/10.5194/acp-18-14095-2018>

909 Zhu, W., Guo, S., Zhang, Z., Wang, H., Yu, Y., Chen, Z., et al. (2021a). Mass spectral characterization of
910 secondary organic aerosol from urban cooking and vehicular sources. *Atmospheric Chemistry and*
911 *Physics*, 21(19), 15065–15079. <https://doi.org/10.5194/acp-21-15065-2021>

912 Zhu, W., Zhou, M., Cheng, Z., Yan, N., Huang, C., Qiao, L., et al. (2021b). Seasonal variation of aerosol
913 compositions in Shanghai, China: Insights from particle aerosol mass spectrometer observations.
914 *Science of The Total Environment*, 771, 144948. <https://doi.org/10.1016/j.scitotenv.2021.144948>

915 Zotter, P., Herich, H., Gysel, M., El-Haddad, I., Zhang, Y., Močnik, G., et al. (2017). Evaluation of the
916 absorption Ångström exponents for traffic and wood burning in the Aethalometer-based source
917 apportionment using radiocarbon measurements of ambient aerosol. *Atmospheric Chemistry and*
918 *Physics*, 17(6), 4229–4249. <https://doi.org/10.5194/acp-17-4229-2017>